Response to anonymous Referee #1

This paper describes a model-measurement comparison study focusing on gaseous oxidized Hg (GOM) in the atmosphere at 3 sites in New Hampshire (marine, coastal, and inland). The main motivation for this study is to use updated reaction mechanisms and physical processes that control concentrations of GOM in the atmosphere and see if the model can reasonably reproduce the observations. There are many gaps in the understanding of what controls GOM in the atmosphere and these gaps are important to close since this species is readily wet and dry deposited and contributes to the burden of Hg accumulation in aquatic and terrestrial ecosystems. The photochemical Hg box model used in this work represents the state of the art with many updated reaction mechanism and physical processes. The sensitivity testing of the model output to changing chemical and physical parameters is very good. The model reproduces the observations reasonably well, the most notable agreement is that the differing overall GOM measured concentrations between sites (AI > TF > PM) is reproduced in the model. The model also gives some indication of which chemical species comprise GOM at the different sites. This is new and valuable information if it can be corroborated by measurements.

We thank the reviewer for their thoughtful, constructive comments and suggestions. The manuscript has been revised carefully. Below we addressed the review point by point.

The main issue overall I have with the paper is that there is little discussion of the GOM measurements made at the 3 sites. At the end of the paper the authors acknowledge the latest papers suggesting that GOM may be systematically underestimated by the Tekran methods, but in the paper the authors do not indicate if there are any potential measurement biases in the data from the 3 sites, and if so how these might change the conclusions reached from the model-measurement comparison. This is a fundamental weakness of such a study that uses measurements with a high degree of uncertainty to validate (or compare to) a model that is also uncertain. That limitation aside, however, there is a great deal of value in such a comparison, and I find this paper to be largely acceptable as-is.

As the reviewer pointed out, the potential uncertainty in ambient Hg measurements especially GOM is a consensus in the community at large. 0Recent laboratory experiments and reviews (Lyman et al., 2010; Jaffe et al., 2014; McClure et al., 2014; Huang and Gustin, 2015; Gustin et al., 2015) reported O_3 and relative humidity (RH) interferences on mercury halides for KCl-coated denuder, which was a part of Tekran 1130 unit used for GOM field measurements commonly in the community as well as the observations of this study. Huang and Gustin (2015) suggested a linear relationship between RH and GOM loss (in %) in GOM measurements, i.e., RH = 0.63 GOM loss % + 18.1, $r^2 = 0.49$, $p < 0.01$, over a RH range of 21% - 62%. In our GOM measurements, the interferences of RH at our three sites should have largely been eliminated since we used a custom-built refrigerator assembly and a canister of drierite to cool and dry air streams before entering into the 1130 pump module (Sigler et al., 2009). As a result, the RH of air streams was kept < 25%, therefore the upper limit of GOM loss caused by RH was < 10% using Huang and Gustin (2015)'s equation.

With regard to O_3 interference, the experimental study (Lyman et al., 2010) showed 3 to 37% reduction on the collection efficiency of $HgCl_2$, and the proposed reaction was $HgCl_2 + 2O_3 \rightarrow Hg^0 + 2O_2 + ClO$. However, a quantitative range of the bias caused by O_3 in field GOM measurements was yet derived (Lyman et al., 2010). Huang et al. (2013) showed lower collection efficiency of KCl denuders compared to nylon membrane and the cation exchange membrane for

$HgBr_2$, $HgCl_2$, HgO, $HgSO_4$, and $Hg(NO_3)_2$ in laboratory tests. However, for field measurements (Huang et al., 2013; Gustin et al., 2013), since GOM and PBM could not be distinguished from total reactive mercury using nylon membrane and cation exchange membrane chambers, the quantitative bias extent derived for total reactive mercury could not be directly used for GOM. Moreover, Huang et al. (2013) suggested that in their marine boundary layer site and highway impacted site, ambient GOM most likely existed in forms other than the laboratory tested species. Therefore, bias low GOM collection efficiency of KCl-coated denuders in field measurements remains speculative at this point.

Quality measurement data are used as ground truth for atmospheric Hg modeling studies, notwithstanding their limitation. Better instrumentation and/or solidly quantified bias for current instruments are in urgent need and are of essential importance to atmospheric Hg modeling. Nevertheless, even if models did not perfectly reproduced observations, the information derived from model simulations and sensitivity studies could provide insight into how the mechanisms work.

Relevant change in revised manuscript: we added a discussion on potential GOM measurement bias and effects on model-measurement comparison in the summary section (lines 623-640).

Abstract: I understand word count in limited, but there should be some indication of what is new or novel about the research. Which finding contributes to our understanding the best? It should be more than a list of observations, but rather some indication of why these observations matter.

The abstract was revised upon the reviewer's suggestion to reflect the findings of the study that are original.

Relevant change in revised manuscript: lines 18-25 were added.

Line 11, Page 3, provide reference(s) for this statement.

Reworded and references added.

Relevant change in revised manuscript: lines 56-58.

Line 20 Page 6, "The ClO /BrO / IO radical cycles involve oxidation of Cl /Br / I radicals, photodissociation of $ClNO_2$ / $ClONO_2$ /$BrNO_2$ /$BrONO_2$, production from other halogen radicals, and sink reactions to reproduce Cl/Br/O radicals or other halides." What is meant by "reproduce"? Do you mean to reproduce the observations? What if those observations are very uncertain?

Changed to "calculate". No observations of Cl, Br and I radicals.

Relevant change in revised manuscript: line 174.

Line 15 Page 10, and Figure 2, there needs to be some discussion about the Tekran measurements. There were no mention of these in the methods section. Were the 3 instruments at the 3 locations operated in a consistent manner? Why such a large variation in GOM at AI, but very low levels at PM? The authors state the MDL for GOM is 0.1 ppqv yet most of the PM data in Figure 2 is < MDL. Hard to make interpretations about the diel cycle of these data since they are so low. Which begs the question, why are they so low at this site?

A brief discussion about the Tekran measurements was added upon the reviewer's suggestion (lines 193 - 200 in the revised manuscript).

GOM was collected over a 2-h sampling period at a rate of 10 L min^{-1} using a speciation unit (Tekran 1130) installed upstream of the total gaseous mercury (TGM) analyzer. The instruments for the three sites were run and calibrated in the lab first and then operated at the sites in a consistent manner. The GOM detection limit for all three instruments were derived as ~0.1 ppqv, based on three times the standard deviation of the averaged blank (Sigler et al., 2009; Mao and Talbot, 2012). We added this information in section 2.1.2.

Pack Monadnock (PM) is a heavily forested, elevated, inland site, representing continental background conditions with nearly no marine influence. PM is not the only site with frequent below LOD measurements of GOM; in fact, similar levels of GOM have been reported from other background sites over the United States (Hall et al., 2006; Engle et al., 2010; Kolker et al., 2010; Choi et al., 2013).

Several possible reasons were proposed to explain significantly lower GOM mixing ratios at PM in comparison with the higher values at AI. First, the GEM oxidation at PM is not as active as that at AI due to a lack of halogen radicals. Second, the dry deposition velocity of GOM at PM (2 cm s^{-1}) was estimated a factor of 3 greater than that at AI (0.5 cm s^{-1}) using the values from Zhang et al. (2009, 2012). Third, the gas-particle partitioning process at PM was favorable for PBM formation, which could be conducive to a high loss rate of GOM. In fact, our model sensitivity runs suggested that the strong oxidation of GEM by O_3 at PM could lead to higher GOM mixing ratios (up to 4 ppqv) during daytime if the same gas-particle partitioning and dry deposition velocity that were used for AI were applied at PM (Figure 6 and Section 3.4.2 in revised manuscript). The simulated production and loss rates of GOM were on average 3.4 molecules cm^{-3} s^{-1} and 5.1 molecules cm^{-3} s^{-1}, respectively, at 0.1 ppqv GOM. The production and loss were balanced out at 0.066 ppqv GOM. This suggests all the GOM produced from GEM oxidation at PM might have been lost rapidly via dry deposition and gas-particle partitioning. Moreover, PM would be in the residual layer at night, with air masses from the preceding daytime convective boundary layer where the GOM concentrations were typically below LOD.

Here we attached detailed information on GOM (also termed as RGM) measurements from Sigler et al. (2009):

*"*RGM is measured with a speciation unit (Tekran model 1130) consisting of a denuder and pump module installed upstream of the TGM analyzer. At TF and PM, the analyzer is housed in a temperature-controlled (~25°C) instrumentation shed. The denuder module is mounted on top of the shed at a height of approximately 5m. At AI, the denuder module is mounted at the top of a World War II-era observation tower (~20m), with the TGM analyzer installed inside the top floor.

The denuder module is attached to the pump module and TGM analyzer by a heated (50°C) umbilical line. The KCl-coated denuder strips out RGM during a predetermined sampling period while the TGM analyzer continuously measures Hg^0 (see Landis et al., 2002). Over the final 30 min of the sampling period, the denuder is flushed with zero air and heated to 500 °C so that the RGM is thermally absorbed and sampled (as Hg^0) by the TGM analyzer. Uncertainty of RGM measurements is high, especially at low levels, and we currently lack standard reference materials for calibration (Aspmo et al., 2005). To reduce uncertainty as much as possible, we strive for very low blanks. We measure RGM over a 2-h sampling period at a rate of 10 L min^{-1}, and with a detection limit of ~0.1 ppqv, based on three times the standard deviation of the averaged blank (e.g., 0.003±0.03 ppqv, n = 3626 at TF in 2007; Sigler et al., 2009).

Clean operation of the 1130 system is verified by flushing the system with zero air. Ideally the resultant mixing ratio during zero air flushes before and after denuder heating is 0 ppqv. To ensure clean operation, the denuders, denuder module glassware, impactor frits and sample filters are replaced and cleaned on a 10-day basis at TF and PM, and typically on a 2-3 week basis at AI. At TF and especially AI, high humidity may corrode zero air canisters, saturate soda lime and lead to poor blanks or enhance cartridge passivation. To minimize the potential of moisture damage and improve blanks during desorption, the airstream leading into the 1130 pump module is cooled and dried using a custom-built refrigerator assembly and a canister of drierite. This system ensures that even when the drierite is exhausted, the relative humidity of the air entering the pump module is ~25% or less. At AI, humidity as well as sea salts led to high blanks during the first month of deployment in 2007. Addition of the refrigerator assembly along with replacement of an aging pump diaphragm on 9 August resulted in clean blank values (0 ppqv) on more than 80% of the RGM observations at AI for the remainder of the field campaign.

In our experience, mixing ratios of 0 ppqv are achieved for > 99% of zero air flushes after desorption and for >94% of zero air flushes immediately before desorption at both TF and PM. When a level of 0 ppqv is not achieved, a blank correction is made to the resultant mixing ratio based on the average value of measurements during zero air flushes before and after desorption."

Relevant change in revised manuscript: lines 193 – 200 were added.

Diel cycles of GOM at AI and TF are consistent with each other with an afternoon maximum, thus the statement on line 17 of Page 10 is misleading.

Deleted this sentence.

Relevant change in revised manuscript: line 267.

Also, time axes in Figure 2 are not perfectly consistent for GOM and GEM. Please fix.

Fixed.

Relevant change in revised manuscript: Figure 2.

Line 10, page 11, without some discussion of instrument intercomparison between the 3 sites, we cannot tell whether a GEM difference of 8% or 12% is simply due to the Tekran or is a real difference.

The instruments for the three sites were run and calibrated in the lab first and then operated at the sites in a consistent manner. Below information on the measurements at the three sites was added in the text (lines 193 - 197 in section 2.1.2 in the revised manuscript):

"For these three sites, the instruments were first run and calibrated in the laboratory and then operated at the sites in a consistent manner. GEM was measured at 5-min intervals and with a limit of detection (LOD) of ~5-10 ppqv (Mao et al., 2008), RGM was measured over a 2-h sampling period with a LOD of ~0.1 ppqv based on three times the standard deviation of the field blank values (Sigler et al., 2009; Mao and Talbot, 2012)."

Relevant change in revised manuscript: lines 193-197 were added.

Line 20, Page 11, the elevation of PM is 700 m asl, but this site is not a mountain peak and thus cannot be above the nocturnal boundary layer consistently. There may be more replenishment of GOM at this site, but again, the levels are super low and as such not much interpretation can be made of the GOM data at this site. In general, I feel the measurements from PM are of little value

to the paper. The AI measurements are of greatest value since they are much higher and also are in the MBL where it appears that Br chemistry probably dominates. I would focus more on the model-measurement comparison at this site and less so on the comparison with the PM data.

We agree that the MBL data are most interesting to understanding Hg chemistry, whereas the GOM mixing ratios at PM appear to be too low for meaningful interpretation if we used the observational data at the site alone. However, in this study, in our opinion it is important to include PM measurements because it could provide a comparison of GOM mixing ratios from three very different environments. Pack Monadnock (PM) is a heavily forested, elevated, inland site, representing continental background conditions with nearly no marine influence. PM is not the only site with frequent below LOD measurements of GOM; in fact, similar levels of GOM have been reported from other background sites over the United States (Hall et al., 2006; Engle et al., 2010; Kolker et al., 2010; Choi et al., 2012).

We agree that interpretation of GOM mixing ratios <LOD would not be of much value. The site comparison was limited largely for the sensitivity runs to determine the processes that could potentially result in such the observed site difference in GOM mixing ratios.

References

Aspmo, K., Gauchard, P.-A., Steffen, A., Temme, C., Berg, T., Bahlmann, E., Banic, C., Dommergue, A., Ebinghaus, R., Ferrari, C., Pirrone, N., Sprovieri, F. and Wibetoe, G.: Measurements of atmospheric mercury species during an international study of mercury depletion events at Ny-Ålesund, Svalbard, spring 2003. How reproducible are our present methods?, Atmospheric Environment, 39(39 SPEC. ISS.), 7607–7619, 2005.

Choi, H.-D., Huang, J., Mondal, S. and Holsen, T. M.: Variation in concentrations of three mercury (Hg) forms at a rural and a suburban site in New York State, Sci. Total Environ., 448, 96–106, doi:10.1016/j.scitotenv.2012.08.052, 2013.

Engle, M. A., Tate, M. T., Krabbenhoft, D. P., Schauer, J. J., Kolker, A., Shanley, J. B. and Bothner, M. H.: Comparison of atmospheric mercury speciation and deposition at nine sites across central and eastern North America, J. Geophys. Res., 115(D18), D18306, doi:10.1029/2010JD014064, 2010.

Gustin, M. S., Amos, H. M., Huang, J., Miller, M. B. and Heidecorn, K.: Measuring and modeling mercury in the atmosphere: a critical review, Atmos. Chem. Phys., 15(10), 5697–5713, doi: 10.5194/acp-15-5697-2015, 2015.

Gustin, M. S., Huang, J., Miller, M. B., Peterson, C., Jaffe, D. A., Ambrose, J., Finley, B. D., Lyman, S. N., Call, K., Talbot, R., Feddersen, D., Mao, H. and Lindberg, S. E.: Do we understand what the mercury speciation instruments are actually measuring? Results of RAMIX, Environmental Science and Technology, 47(13), 7295–7306, 2013.

Hall, B. D., Olson, M. L., Rutter, A. P., Frontiera, R. R., Krabbenhoft, D. P., Gross, D. S., Yuen, M., Rudolph, T. M. and Schauer, J. J.: Atmospheric mercury speciation in Yellowstone National Park, Science of The Total Environment, 367(1), 354–366, doi:10.1016/j.scitotenv.2005.12.007, 2006.

Huang, J. and Gustin, M. S.: Uncertainties of Gaseous Oxidized Mercury Measurements Using KCl-Coated Denuders, Cation-Exchange Membranes, and Nylon Membranes: Humidity Influences, Environ. Sci. Technol., 49(10), 6102–6108, doi:10.1021/acs.est.5b00098, 2015.

Huang, J., Miller, M. B., Weiss-Penzias, P. and Gustin, M. S.: Comparison of gaseous oxidized Hg measured by KCl-coated denuders, and nylon and cation exchange membranes, Environmental Science and Technology, 47(13), 7307–7316, 2013.

Jaffe, D. A., Lyman, S., Amos, H. M., Gustin, M. S., Huang, J., Selin, N. E., Levin, L., ter Schure, A., Mason, R. P., Talbot, R., Rutter, A., Finley, B., Jaeglé, L., Shah, V., McClure, C., Ambrose, J., Gratz, L., Lindberg, S., Weiss-Penzias, P., Sheu, G.-R., Feddersen, D., Horvat, M., Dastoor, A., Hynes, A. J., Mao, H., Sonke, J. E., Slemr, F., Fisher, J. A., Ebinghaus, R., Zhang, Y. and Edwards, G.: Progress on Understanding Atmospheric Mercury Hampered by Uncertain Measurements, Environ. Sci. Technol., 48(13), 7204–7206, doi:10.1021/es5026432, 2014.

Kolker, A., Olson, M. L., Krabbenhoft, D. P., Tate, M. T. and Engle, M. A.: Patterns of mercury dispersion from local and regional emission sources, rural Central Wisconsin, USA, Atmos. Chem. Phys., 10(10), 4467–4476, doi:10.5194/acp-10-4467-2010, 2010.

Landis, M. S., Stevens, R. K., Schaedlich, F. and Prestbo, E. M.: Development and characterization of an annular denuder methodology for the measurement of divalent inorganic reactive gaseous mercury in ambient air, Environ. Sci. Technol., 36(13), 3000–3009, 2002.

Lyman, S. N., Jaffe, D. A. and Gustin, M. S.: Release of mercury halides from KCl denuders in the presence of ozone, Atmos. Chem. Phys., 10(17), 8197–8204, doi:10.5194/acp-10-8197-2010, 2010.

Mao, H., Talbot, R. W., Sigler, J. M., Sive, B. C. and Hegarty, J. D.: Seasonal and diurnal variations of Hg° over New England, Atmospheric Chemistry and Physics, 8(5), 1401–1421, 2008.

Mao, H. and Talbot, R.: Speciated mercury at marine, coastal, and inland sites in New England-Part 1: Temporal variability, Atmospheric Chemistry and Physics, 12(11), 5099–5112, 2012.

McClure, C. D., Jaffe, D. A. and Edgerton, E. S.: Evaluation of the KCl Denuder Method for Gaseous Oxidized Mercury using HgBr2 at an In-Service AMNet Site, Environ. Sci. Technol., 48(19), 11437–11444, doi:10.1021/es502545k, 2014.

Sigler, J. M., Mao, H. and Talbot, R.: Gaseous elemental and reactive mercury in Southern New Hampshire, Atmos. Chem. Phys., 9(6), 1929–1942, doi:10.5194/acp-9-1929-2009, 2009.

Zhang, L., Wright, L. P. and Blanchard, P.: A review of current knowledge concerning dry deposition of atmospheric mercury, Atmospheric Environment, 43(37), 5853–5864, 2009.

Zhang, L., Blanchard, P., Johnson, D., Dastoor, A., Ryzhkov, A., Lin, C. J., Vijayaraghavan, K., Gay, D., Holsen, T. M., Huang, J., Graydon, J. A., Louis, V. L. S., Castro, M. S., Miller, E. K., Marsik, F., Lu, J., Poissant, L., Pilote, M. and Zhang, K. M.: Assessment of modeled mercury dry deposition over the Great Lakes region, Environmental Pollution, 161, 272–283, 2012.

Response to anonymous Referee #2

The authors present results of a box-model simulation of Hg chemistry at three sites in southern New Hampshire, USA. The sites are located in different environments (marine, coastal, and elevated), which allows the authors to examine the similarities and differences in Hg chemistry in these environments. The authors conclude that Br and BrO dominate Hg oxidation during the day and H_2O_2 at night at the marine site, while O_3 and OH are dominant at the coastal and inland sites. I found the comparison in Hg chemistry between the sites interesting. Atmospheric Hg chemistry remains one of the least understood processes controlling Hg cycling in the environment. Studies like this that use models to interpret in situ Hg observations in different environments are necessary to fully characterize the oxidation of Hg in the atmosphere. However, I have a number of major concerns that the authors should address to make their study convincing.

We thank the reviewer for their detailed, thoughtful, constructive comments and suggestions. The manuscript has been revised carefully. Below we addressed the review point by point.

Major comments: 1) The authors examine the oxidation of GEM with the set of gas phase reactions listed in Table 1. There is high uncertainty in these reaction rates, up to a factor of 10 for reactions of GEM with Br and BrO. The recent review by Ariya et al. (2015) has a compilation of all previously reported estimates for GEM oxidation reaction rates. The authors perform one sensitivity study addressing the uncertainty in the GEM+O_3 rate, but seem to ignore the uncertainty in the remaining reactions. A discussion of the effect of these uncertainties are necessary before any conclusion can be reached about the dominant GEM oxidation pathways at the studies sites.

The major oxidation reactions of GEM are GEM + O_3 and GEM + Br in our box model. For the GEM + Br reaction, Ariya et al. (2002) yielded a rate constant of 3.2×10^{-12} cm^3 $molecule^{-1}$ s^{-1} using a relative rate method. However, Ariya et al. (2002) used one single rate reference only, which largely limited the accuracy of their results (Hynes et al. 2009). Moreover, large amounts of cyclohexane (an OH scavenger) used in Ariya et al. (2002)'s experiment may lead to an enhancement in the absorption of reactants on the cell walls (Hynes et al. 2009). A number of studies (Spicer et al. 2002; Donohoue et al. 2006; Sumner et al. 2011; Subir et al., 2011; Goodsite et al., 2004, 2012) showed a narrow range of $(3.0 – 6.4) \times 10^{-13}$ cm^3 $molecule^{-1}$ s^{-1} for the rate coefficient of GEM + Br, from which we used a temperature dependent rate coefficient of $3.7 \times 10^{-13}(T/298)^{-2.76}$ cm^3 $molecule^{-1}$ s^{-1} from Goodsite et al. (2004; 2012). To further investigate the GEM + Br rate coefficient sensitivity on GOM simulation, we added a new sensitivity scenario using Ariya et al. (2002) rate coefficient (section 3.4.1 in the revised manuscript). As a result, using the greater rate coefficient of Ariya et al. (2002) produced a factor of 3 or higher GOM mixing ratios than the base scenario.

We added the following discussion on the effect of reaction kinetics uncertainties on model simulations in section 3.4.1 (lines 522 - 527) of revised manuscript:

"Using a slower rate coefficient of GEM + O_3 (Hall, 1995) had similar effects as not including the GEM + O_3 reaction, i.e. decreasing GOM mixing ratios, especially at nighttime, and brominated GOM species becoming dominant. The GEM + OH reaction was not as important as GEM + O_3 or Br. The use of a higher GEM + Br rate coefficient derived from the study by Ariya et al. (2002) caused more than a factor of 3 higher GOM and PBM resulting in overestimated GOM for most cases."

Relevant change in revised manuscript: we added a sensitivity scenario in section 3.4.1, see changes in line 488, lines 504-506, and Table 3 (scenario 9). A discussion on effects of GOM oxidation reactions uncertainties were added in lines 522-527.

2) How were the concentrations of the species that weren't measured set? How were the concentrations of Br/Cl/I species determined at the three sites? The authors briefly mention this in Section 3.4.1. This is a key aspect of the study and should be discussed in detail in Section 2.

For species that were not measured, we use the chemical mechanism to calculate their concentrations. Initial concentrations of most unmeasured species were set as the values in similar environments from the literature if available. Br/Cl/I concentrations were all calculated from the model given initial concentrations of 1 pptv (e.g. Finley et al., 2008; except for AI) for Br_2, Cl_2, and I_2 species. At AI, we set the Br_2 concentration to be constant during simulations and used Saiz-Lopez et al. (2006)'s values to constrain [BrO]. At TF and PM, the initial concentrations of Br_2, Cl_2, and I_2 were not sensitive factors for the simulated concentrations of Br/Cl/I, because during the simulations, Br_2, Cl_2, and I_2 were rapidly depleted without sources in inland environments.

We have added such information in section 2.1.2 (lines 189-191 and 203 - 207 in the revised manuscript) as follows:

"For species that were not measured, we set their initial concentrations as the values in similar environments from the literature if available."

"Br/Cl/I concentrations were all calculated from the model given initial concentrations of 2 pptv (Finley et al., 2008; except for AI) for Br_2, Cl_2, and I_2 species. At AI, the Br_2 initial concentration was set to be constant during simulations and used Saiz-Lopez et al. (2006)'s values to constrain [BrO]. Detailed information can be found in Section 3.3.1."

Relevant change in revised manuscript: lines 189-191, and lines 203-207.

3) The authors performed several sensitivity studies with the box-model by varying different physical and chemical parameters. However, these sensitivity studies seem out of place. The authors do not specify why they chose to vary the parameters listed in Table 3, and not others. Secondly, the presentation of the results of the sensitivity studies is not thorough. There is no discussion of how the results of the sensitivity studies affect the overall conclusions. Section 3.3.3 addresses Br chemistry in the MBL. I do not think this fits in this study, considering that there were no BrO measurements that could be used to compare with the model results.

The ranges of parameters in sensitivity studies were based upon the varying range of each parameter from observations and the literature. The liquid water content range was derived from Hedgecock et al. (2003). The temperature range was based on the magnitude of observed average temperature diurnal cycles. We added such information in section 3.4.1 of revised manuscript (lines 487 - 490).

More discussion on the effect of these sensitivity tests was added (lines 518 - 530 in the revised manuscript):

"In summary, the parameters used in gas-particle partitioning processes including solar radiation values, temperature, and the rate coefficients of major GEM oxidation reaction, could all affect simulated GOM mixing ratios but with varying degrees. Aerosol properties were suggested to play a very important role in the partitioning of ambient GOM and PBM species and thus should be better represented in future Hg model simulation studies. Using a slower rate coefficient of

GEM + O_3 (Hall, 1995) had similar effects as not including the GEM + O_3 reaction, i.e. decreasing GOM mixing ratios, especially at nighttime, and brominated GOM species becoming dominant. The GEM + OH reaction was not as important as GEM + O_3 or Br. The use of a higher GEM + Br rate coefficient derived from the study by Ariya et al. (2002) caused more than a factor of 3 higher GOM and PBM concentrations resulting in overestimated GOM for most cases. GOM and PBM production appeared to favor lower temperature during daytime and higher temperature at night, and simulated GOM concentrations were not as sensitive to temperature change as to solar radiation and gas-particle partitioning."

Regarding section 3.3.3 (section 3.4.3 in the revised manuscript), in our opinion, this is one of the original contributions this study offers. Considering the importance of halogen chemistry in Hg cycling, we think halogen chemistry needs to be interactive with Hg chemistry. Constraining the BrO simulations using the observations from Saiz-Lopez et al. (2006), our box model results suggested that Br and BrO are two key compounds in determining GOM mixing ratios in the MBL. Section 3.4.3 in the revised manuscript includes theoretical analysis and discussion of the important bromine reactions that could affect Br and BrO simulations, which has vital importance in this study and can provide guidance for future Hg studies.

Relevant change in revised manuscript: lines 487-490 and lines 518-530.

4) Hg^{2+} reduction reactions were included in the model. Is reduction an important control on GOM mixing ratios? Some discussion of the effect of the reduction pathways on GOM and PBM would be valuable. The Tekran 2537/1130/1135 typically measures GEM, RGM, and PBM. The PBM measurements are not discussed in the manuscript. Can the PBM measurements be used to constrain the reduction rates?

A table with aqueous Hg reactions used in our model was added as Table S1.

Aqueous Hg reduction is one of the major sources of GEM in the atmosphere. Therefore, aqueous Hg reactions is supposedly a factor controlling GEM mixing ratios and further influence GOM mixing ratios. However, in this study aqueous Hg reduction was not an important control on GOM simulations. This is because GEM mixing ratios in the model were fixed using observed values. The uncertainties associated with aqueous Hg reactions would not influence GEM mixing ratios and therefore have minor effects on simulated GOM mixing ratios.

It is true that high quality GOM and PBM measurements would be of great help for modelling studies to evaluate the schemes such as gas-particle partitioning process as well as to constrain the aqueous reduction rate. However, the inlet of the Tekran speciation sampling system had an elutriator inlet with an acceleration jet to remove aerosols > 2.5 μm so that only PBM on fine particles was measured. The PBM calculated from the box model does not include size fractionation, thus Tekran $PBM_{2.5}$ measurements could not be used to constrain our simulations and the reduction rate.

Relevant change in revised manuscript: Table S1 was added.

5) In Section 1, the authors briefly discuss previous studies of Hg chemistry by Hedgecock et al., Holmes et al., and Wang et al. The present study of Ye at al. is very similar to these previous studies. All of them examine the diurnal cycle of oxidized Hg in the mid-latitude marine boundary layer using a box-model. The authors should include a discussion of how their results compare with the findings in these previous studies.

Section 1 was revised and expanded to reflect the aspects of this study that differentiate it from previous studies.

Relevant change in revised manuscript: lines 119-121 and lines 131-141.

Minor comments: Page 4, line 9: "Hg in the MBL cycles differently in coastal or inland areas." The difference needs to be expanded upon as this is directly related to the present study. How is the cycle different?

The major differences of Hg cycles between MBL and coastal or inland areas are reflected in the magnitude and speciation of GOM, which are due to different chemical, meteorological and atmospheric conditions such as halogen radical mixing ratios, boundary layer height, and atmospheric particles size and properties. More detailed discussion can be found in section 3.1 and section 3.4.2 in the revised manuscript.

Page 5, line 23: Please add a list of reactions and their rates as a supplement, given that a few of the reactions do not seem to follow the JPL Report #17 recommendations.

We have 424 reactions in total, which is too many to be included in the publication. We would be happy to provide the reactions upon request.

Halogen reactions listed in Table 4 were following the halogen chemistry reviews by Atkinson et al. (2004; 2008). We added this information in section 2.

Relevant change in revised manuscript: line 155.

Page 6, line 11: Please include a table with the reaction rates and references for the aqueous-phase reactions.

A table showing aqueous Hg reactions in our model was added as Table S1.

Relevant change in revised manuscript: Table S1 was added.

Page 7, line 1: Not all previous modeling studies have used simple approximations. The model of Hedgecock et al. (2003, 2005) uses detailed MBL chemistry.

The sentence has been revised.

Relevant change in revised manuscript: line 178.

Page 7, line 11: How are the wind speed measurements used in the box-model?

Wind speed measurements were used for case selection, not input for the box model. The text was revised to reflect this.

Relevant change in revised manuscript: line 188.

Page 7, line 19: "...were set to be constant during a simulation." Please specify the length of a simulation. Was it one day or one hour?

The length of a simulation is one hour. The sentence was revised to include this.

Relevant change in revised manuscript: line 203.

Page 9, line 20: It would be interesting to see how the source regions of the air masses at the three sites differed. The back trajectories for only the AI site are discussed in the text.

The back trajectories for the PM and TF sites (Fig. 1) showed air masses source regions. Air masses reaching PM originated from inland areas west to north of the site, while air masses at TF half came from northwestern to northern inland areas and half from the marine boundary layer. However, we did not find correlation between source regions and GOM mixing ratios at TF and PM. This is why the origin of air masses at the two sites was not discussed.

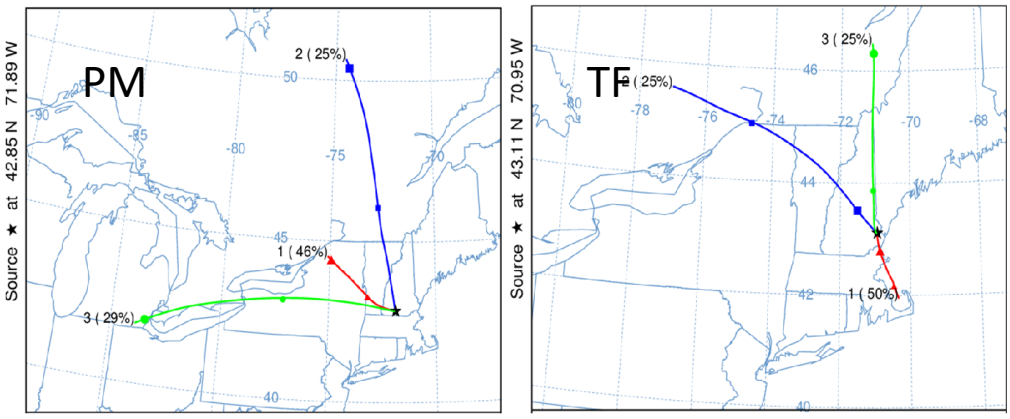

Figure 1. Clustered 24-hour backward trajectories of air masses in all cases at PM and TF.

Page 10, line 21: The LOD for the GOM observations was 0.1 ppqv at AI, but it appears to be much lower at PM. Figure 2 shows most GOM observations at PM below 0.05 ppqv. Please specify the LOD for GOM at PM.

The GOM detection limit for all three instruments were derived as ~0.1 ppqv, based on three times the standard deviation of the averaged blank (Sigler et al., 2009; Mao and Talbot, 2012). We added this information in section 2.1.2.

Relevant change in revised manuscript: lines 194-197.

Page 12, line 12: HgO is considered a GOM species here, although the authors state in the Introduction (page 3, line 22) that "a consensus has emerged that GEM+O_3 reaction most likely occurs with solid-phase products..."

The experimental study by Pal and Ariya (2004) measured 1% of HgO produced by GEM + O_3 on an aerosol filter. Snider et al. (2008) showed HgO(s) production in their kinetic and product study. A theoretic study of Schroeder et al. (1998) suggested HgO would not exist as an isolated molecule at a decomposition temperature of +500 °C. However, the GEM + O_3 reaction and decomposition temperature (Schroeder et al., 1998) could also be impacted by the presence of other ambient gases (Snider et al., 2008; Gustin et al., 2013; Seigneur et al., 1994). Moreover, a recent study by Huang et al. (2013) observed gas-phase HgO using nylon and cation exchange membranes. Overall our knowledge about this reaction remains nebulous. We added this discussion in the introduction (section 1).

Relevant change in revised manuscript: lines 67-79.

Page 12, line 19, I was surprised not to see $HgBrNO_2$ as one of the more abundant GOM species. I expected $HgBrNO_2$ to be produced faster than HgBrOOH and Hg-BrOBr, given the typically higher concentrations of NO_2.

In checking reactions forming $HgBrNO_2$, we found a mistake in NO_x input. We should have fixed NO_x concentrations in the input for the simulations but it was mistakenly left unfixed. In this revised version, we have rectified the mistake. As a result, the dominant brominated GOM species was changed to $HgBrNO_2$, and following with HgBrO; other brominated GOM species were negligible. However, Hg+Br reaction is so slow compared to further HgBr oxidation reactions that Hg+Br is the rate-limiting step for these two steps of reactions. Therefore, the change in the total GOM production was minor, and major conclusions remain unchanged (See Section 3.2 in the revised manuscript).

Relevant change in revised manuscript: lines 33-34, lines 301-303, lines 307-309, lines 312-316, lines 338-340, lines 423-425, lines 443-449, lines 4662-463, line 496, Table 2, Table 3, Figures 2-8 (except for Figure 5) were changed to reflect the new simulation results.

Page 13, line 14: Why were HgO and $Hg(OH)_2$ more sensitive than halogenated GOM species to gas-particle partitioning?

The difference between sensitivity of $HgO/Hg(OH)_2$ and halogenated GOM species to gas-particle partitioning was caused by higher molar mass of halogenated GOM species than $HgO/Hg(OH)_2$. When taken into calculations, compounds with smaller molar mass had a higher gas-to-particle rate based on the scheme described in section 2.1.3. The Henry's constant values of $Hg(OH)_2$ and halogenated GOM species are large enough to be not as sensitive as the molar mass of the compounds is to gas-to-particle partitioning.

Page 24, line 25: I do not see an order of magnitude difference between the peaks in Figure 5. I see a factor of 2-3 difference.

Corrected.

Relevant change in revised manuscript: line 546.

Page 19, lines 12 onwards: Could entrainment from the free troposphere explain this inverse relation between GOM and RH? Entrainment from the free troposphere was not treated explicitly, yet the boundary layer height at the TF site varied diurnally. Was it assumed that this entrainment does not change GOM mixing ratios in the boundary layer?

In this study, we selected clear-sky and calm wind conditions, usually accompanied by strong stability with a strong inversion layer at the top of the daytime convective PBL layer based on measurements from the literature (e.g., Hogan et al., 2009). Minimal entrainment at the top of the boundary layer was thus expected.

We agree with the reviewer's point that at TF, the GOM in the remnant layer could be mixed down to the surface in the morning when the boundary layer rises. The observed daytime GOM mixing ratio peak is around 0.8 ppqv, and the contribution of downward mixing from the remnant layer at TF was estimated by Mao et al. (2006) to be about ~23% in the time window of after sunrise and 10 am local time. Under such circumstances, the contribution from the preceding convective boundary layer to the morning GOM mixing ratios would at most be ~0.2 ppqv. Moreover, even though GOM in the remnant layer at night did not deposit to the surface, it could be lost by deposition to aerosols and via other unknown mechanisms. Taking these into consideration, that 0.2 ppqv contribution from the remnant layer would be the upper limit. As the day progresses and solar radiation gets stronger, the GOM mixing ratio is mostly driven by photochemical production.

Page 21, line 29: "Clearly, the under-estimation case occurred under the strongest Bermuda High influence..." It isn't clear to me. Can the authors explain a bit more why it is the influence of the Bermuda High, and not just a transient high-pressure system?

The under-estimation cases were 06/13/2008 and 08/22/2007, the meteorological conditions of these days were illustrated using the NCEP 1° x 1° meteorological reanalysis data (Fig. 2). The observed GOM concentrations peaked at 14:00 LT on 06/13/2008 and 16:00 LT on 08/22/2007 respectively. On 13 June 2008, the Bermuda high pressure system covered almost the entire eastern US coastline, where our sites are located. This high pressure system lasted 4 days (10 – 14 June 2008). On 22 August 2007, the continental part of the Bermuda high pressure system was over the southeastern US extending to the northeast. These lasting high pressure systems caused regional buildup pollutants, explaining the observed high mixing ratios of GOM in the two cases. We will include these figures in the supplemental material.

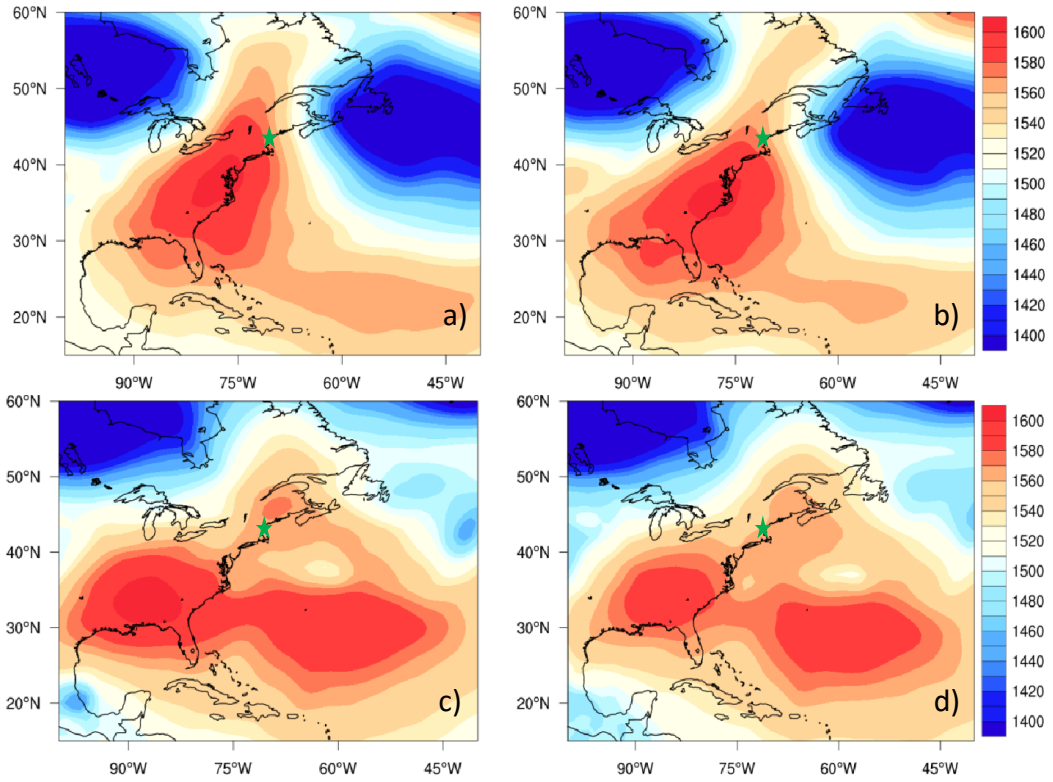

Figure 2. Geopotential height for a) 06/13/2008 08:00 EDT, b) 06/13/2008 14:00 EDT, c) 08/22/2007 14:00 EDT, and d) 08/22/2007 20:00 EDT at 850 hPa, the green star shows the location of TF site.

Relevant change in revised manuscript: lines 451-452; Figure S1 was added.

Page 23, line 7: "It was hypothesized that..." This was not substantiated in the study, and does not belong in the conclusions.

These hypotheses were developed based on the modeling and analysis work in the paper. The text was revised to reflect the logical steps to take to arrive at the hypotheses.

Relevant change in revised manuscript: lines 607-608.

Page 23, line 24: The authors allude to problems in GOM measurements using the Tekran instrument. If the measured GOM is indeed biased low by a factor of 2 or 3 under certain conditions,

how does it affect this study's conclusions? This is important and needs to be discussed in a little more detail.

Page 23: The authors should also point out to the reader that, in the absence of speciated measurements of oxidized Hg compounds, the results of a modeling study cannot be used to conclusively identify the dominant oxidants of Hg in the atmosphere.

The reviewer raised excellent points here. We agree that without measurements of speciated GOM, modeling results cannot be used to conclusively identify the dominant oxidants of Hg, as well as dominant GOM species in that matter, in the atmosphere. Indeed the potential uncertainty in ambient Hg measurements especially GOM is a major concern in the community. We had some discussion on the effect of uncertainty in GOM measurements on our interpretation of measurements data. With the reviewer's suggestion in mind, the discussion was expanded to discuss the potential effect of biased low GOM measurements on our conclusions in the last section (lines 623 - 640 in the revised manuscript).

That being said, it is unlikely to put any range on the bias of our GOM concentrations considering our own GOM measurements and the literature. Recent laboratory experiments and reviews (Lyman et al., 2010; Jaffe et al., 2014; McClure et al., 2014; Huang and Gustin, 2015; Gustin et al., 2015) reported O_3 and relative humidity (RH) interferences on mercury halides for KCl-coated denuder, which was a part of Tekran 1130 unit used for GOM field measurements commonly in the community as well as the observations of this study. Huang and Gustin (2015) suggested a linear relationship between RH and GOM loss (in %) in GOM measurements, i.e., RH = 0.63 GOM loss % + 18.1, $r^2 = 0.49$, $p < 0.01$, at RH range of 21 to 62%. In our GOM measurements, the interferences of RH at our sites should have largely been eliminated since we used a custom-built refrigerator assembly and a canister of drierite to cool and dry air streams before entering into the 1130 pump module (Sigler et al., 2009). As a result, the RH of air streams was kept < 25%, therefore the upper limit of GOM loss cause by RH was < 10% using Huang and Gustin (2015)'s equation.

With regard to O_3 interference, the experimental study (Lyman et al., 2010) showed 3 to 37% reduction on the collection efficiency of $HgCl_2$, and the proposed reaction was $HgCl_2 + 2O_3 \rightarrow Hg^0 + 2O_2 + ClO$. However, the quantitative extent of the bias caused by O_3 in field GOM measurements was yet derived (Lyman et al., 2010). Huang et al. (2013) showed lower collection efficiency of KCl denuders compared to nylon membrane and the cation exchange membrane for $HgBr_2$, $HgCl_2$, HgO, $HgSO_4$, and $Hg(NO_3)_2$ in laboratory tests. However, for field measurements (Huang et al., 2013; Gustin et al., 2013), since GOM and PBM could not be distinguished from total reactive mercury using nylon membrane and cation exchange membrane chambers, the quantitative bias extent derived for total reactive mercury could not be directly used for GOM. Moreover, Huang et al. (2013) suggested that in their marine boundary layer site and highway impacted site, ambient GOM most likely existed in forms other than the laboratory tested species. Therefore, bias low GOM collection efficiency of KCl-coated denuders in field measurements remains speculative at this point.

Quality measurement data are used as ground truth for atmospheric Hg modeling studies, notwithstanding their limitation. Better instrumentation and/or solidly quantified bias for current instruments are in urgent need and are of essential importance to atmospheric Hg modeling. Nevertheless, even if models did not perfectly reproduced observations, the information derived

from model simulations and sensitivity studies could provide insight into how the mechanisms work.

The discussion added in the Summary section is as follows (lines 623 - 640 in the revised manuscript):

"It should be noted that without measurements of speciated GOM, modeling results cannot be used to conclusively identify the dominant oxidants of Hg, as well as dominant GOM species in that matter, in the atmosphere. Indeed, the potential uncertainty in ambient Hg measurements especially GOM is a major concern in the community. That being said, it is unlikely to have a quantitative understanding of the bias of our GOM concentrations. Recent laboratory experiments and reviews (Lyman et al., 2010; Jaffe et al., 2014; McClure et al., 2014; Huang and Gustin, 2015; Gustin et al., 2015) reported O_3 and relative humidity (RH) interferences on mercury halides for KCl-coated denuder, the part of Tekran 1130 unit commonly used for GOM field measurements. As stated in Section 2, in our GOM measurement the RH effect was minimized by adding refrigeration to remove excess of water in the airsteam. O_3 interference and bias low GOM collection efficiency of KCl-coated denuders were limited to a handful of GOM species in laboratory experiments and remain untested in field measurements. If the measured GOM concentrations were indeed biased low by a factor of 2 or 3 under certain conditions as previous studies speculated, the matching cases at AI and TF would be reduced from 50% of the total cases to 30%, and the model would potentially underestimate GOM concentrations in the remaining cases (70%) by a factor of 3 to 4. It is however hard to speculate the effect at PM since most GOM observations there were below the LOD. This suggested even greater unknowns in our understanding of Hg chemistry."

Relevant change in revised manuscript: lines 623-640.

Table 2: Please include the standard deviation of the observed variables.

Added the standard deviation values for observed variables in Table 2.

Relevant change in revised manuscript: Table 2.

Figure 1: Please add some geographical context to the map. May be show the latitude/ longitude girds, and the land/ocean boundary.

Plotted a new map for Figure 1 (Fig. 3 showing below) with latitude/longitude grids and land/ocean boundary showed.

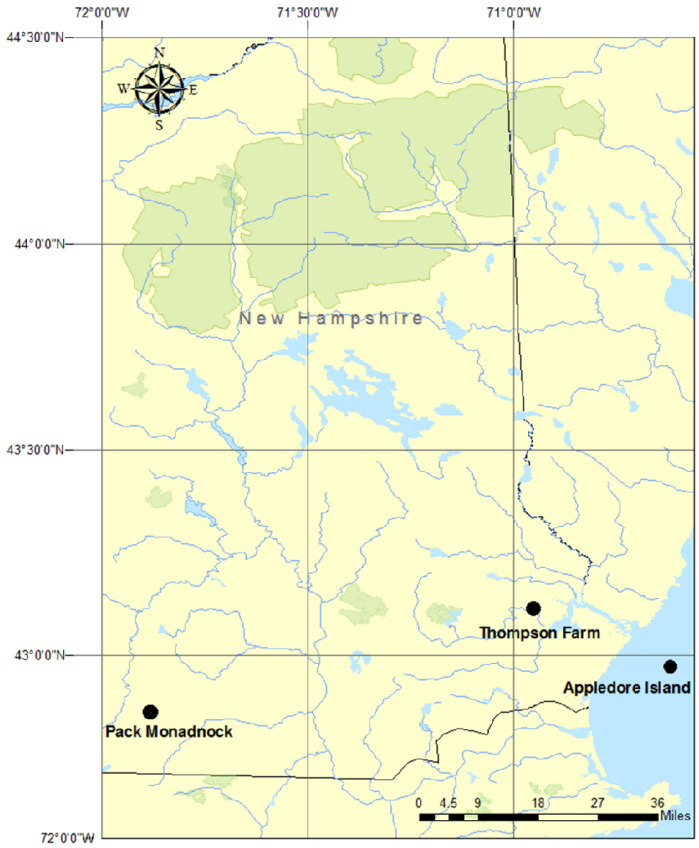

Figure 3. New Hampshire site map: Appledore Island (marine), Thompson Farm (coastal), and Pack Monadnock (inland elevated).

Relevant change in revised manuscript: Figure 1.

Figure 10: The back trajectories suggest strong regional influence at the AI site. Can the authors reconcile this with their assumption for the box-model that regional transport is negligible?

The trajectories were used to identify the origin of the air mass reaching AI. GEM was long-lived enough to originate from the same source region of the air mass. However, GOM in the air masses did not necessarily originate from the same source region due to its short lifetime. Under the conditions of strong atmospheric stability as selected in this study, GOM would likely be in-situ, photochemically produced.

Technical comments: Page 1, line 14: May be the title can specify that the study focuses on the summertime.

Upon the reviewer's suggestion the title was changed to "Investigation of processes controlling summertime gaseous elemental mercury oxidation at mid-latitudinal marine, coastal, and inland sites".

Relevant change in revised manuscript: line 1

Page 1, line 14: The term Hg(II) is not needed here.

Deleted.

Relevant change in revised manuscript: line 34

Page 3, line 7-8. “GOM and PBM are...subject to dry and wet deposition...” GEM is also subject to dry deposition.

Added.

Relevant change in revised manuscript: line 53.

Page 3, line 27: The sentence starting with “In the MBL...” needs to be rephrased for clarity.

Revised.

Relevant change in revised manuscript: lines 81-86.

Page 5, line 10: “...initial GEM mixing ratios...were set to be constant mimicking GEM emission flux.” This sentence is unclear and should be reworded. I think removing the clause “and were set...” may help.

Revised.

Relevant change in revised manuscript: lines 130-136.

Page 10, line 4: FB is fractional bias.

Changed.

Relevant change in revised manuscript: line 255.

Page 11, line 26: Reference to Section 3.2.2. Should this refer to Section 3.4?

In this sentence, we meant that the reasons of large variations of GOM daytime peaks between AI, TF, and PM. We have discussed this in Section 3.4.2 of revised manuscript. We have corrected this.

Relevant change in revised manuscript: line 295.

Page 14, line 15: It seems TF_AIdry, PM_AIdry, TF_AIaero, PM_AIaero are not discussed any further. It would be better to not introduce them here.

Deleted.

Relevant change in revised manuscript: lines 536-540.

Page 17, line 1: I think it would be more appropriate to place the model evaluation section before the sensitivity studies.

Agreed and done.

Relevant change in revised manuscript: In revised manuscript, 3.3 is “Model evaluation”, and 3.4 is “Sensitivity analysis”.

Page 19, line 27: “It was thus hypothesized that certain processes...” This sentence is vague. Please reword.

Revised.

Relevant change in revised manuscript: lines 396-398.

Page 23, line 15: “The updated chemical mechanism largely improved GOM simulations...”. Improved with respect to what?

Revised to “The updated chemical mechanism largely improved the simulation of the magnitude and pattern of GOM diurnal variation at the coastal and inland sites.”

Relevant change in revised manuscript: lines 615-616.

Figure 2: What do the “filled circles” represent? Expand the site abbreviations in the caption. The font size is too small.

The figure was revised.

Relevant change in revised manuscript: Figure 2 was changed.

Figure 3: Font size is too small. In the caption: do the bars “represent” the range of simulated GOM?

The figure was revised and the font size was increased for better presentation. Now the bars represent standard deviations of simulated GOM.

Relevant change in revised manuscript: Figure 3 was merged to Figure 2 in revised manuscript.

Figure 4: Please change “Other_RGM” to “Other GOM species”. Please increase font size. It is hard to distinguish between the lines in Figure 3(a).

Changed.

Relevant change in revised manuscript: Figure 3 in revised manuscript.

Figure 8: Caption: “(“Observed”, red, “Simulated”, triangle)”. Please correct typographical error.

Corrected.

Relevant change in revised manuscript: Figure 8 was merged to Figure 2 in revised manuscript.

Figure 9: It is difficult to distinguish between the Simulated_under-estimated, Simulated_matching, and Simulated_over-estimated lines. It would be also be helpful to maintain consistency between the figures in what is represented by the error bars.

We revised the figures and used error bars for standard deviation only.

Relevant change in revised manuscript: Figure 4 in revised manuscript.

References

Ariya, P. A., Khalizov, A. and Gidas, A.: Reactions of gaseous mercury with atomic and molecular halogens: Kinetics, product studies, and atmospheric implications, Journal of Physical Chemistry A, 106(32), 7310–7320, 2002.

Atkinson, R., Baulch, D. L., Cox, R. A., Crowley, J. N., Hampson, R. F., Hynes, R. G., Jenkin, M. E., Rossi, M. J., Troe, J. and Wallington, T. J.: Evaluated kinetic and photochemical data for atmospheric chemistry: Volume IV – gas phase reactions of organic halogen species, Atmos. Chem. Phys., 8(15), 4141–4496, doi:10.5194/acp-8-4141-2008, 2008.

Donohoue, D. L., Bauer, D., Cossairt, B. and Hynes, A. J.: Temperature and pressure dependent rate coefficients for the reaction of Hg with Br and the reaction of Br with Br: A pulsed laser photolysis-pulsed laser induced fluorescence study, Journal of Physical Chemistry A, 110(21), 6623–6632, 2006.

Finley, B. D. and Saltzman, E. S.: Observations of Cl_2, Br_2, and I_2 in coastal marine air, J. Geophys. Res., 113(D21), D21301, doi:10.1029/2008JD010269, 2008.

Goodsite, M. E., Plane, J. M. C. and Skov, H.: A Theoretical Study of the Oxidation of Hg^0 to $HgBr_2$ in the Troposphere, Environmental Science and Technology, 38(6), 1772–1776, 2004.

Goodsite, M. E., Plane, J. M. C. and Skov, H.: Correction to A Theoretical Study of the Oxidation of Hg^0 to $HgBr_2$ in the Troposphere, Environ. Sci. Technol., 46(9), 5262–5262, doi:10.1021/es301201c, 2012.

Gustin, M. S., Amos, H. M., Huang, J., Miller, M. B. and Heidecorn, K.: Measuring and modeling mercury in the atmosphere: a critical review, Atmos. Chem. Phys., 15(10), 5697–5713, doi: 10.5194/acp-15-5697-2015, 2015.

Gustin, M. S., Huang, J., Miller, M. B., Peterson, C., Jaffe, D. A., Ambrose, J., Finley, B. D., Lyman, S. N., Call, K., Talbot, R., Feddersen, D., Mao, H. and Lindberg, S. E.: Do we understand what the mercury speciation instruments are actually measuring? Results of RAMIX, Environmental Science and Technology, 47(13), 7295–7306, 2013.

Hall, B.: The gas phase oxidation of elemental mercury by ozone, Water Air Soil Pollut., 80(1-4), 301–315, 1995.

Hedgecock, I. M., Pirrone, N., Sprovieri, F. and Pesenti, E.: Reactive gaseous mercury in the marine boundary layer: Modelling and experimental evidence of its formation in the Mediterranean region, Atmos.Environ., 37(SUPPL. 1), S41–S49, 2003.

Hogan, R. J., Grant, A. L. M., Illingworth, A. J., Pearson, G. N. and O'Connor, E. J.: Vertical velocity variance and skewness in clear and cloud-topped boundary layers as revealed by Doppler lidar, Q.J.R. Meteorol. Soc., 135(640), 635–643, doi:10.1002/qj.413, 2009.

Holmes, C. D., Jacob, D. J., Mason, R. P. and Jaffe, D. A.: Sources and deposition of reactive gaseous mercury in the marine atmosphere, Atmospheric Environment, 43(14), 2278–2285, 2009.

Huang, J. and Gustin, M. S.: Uncertainties of Gaseous Oxidized Mercury Measurements Using KCl-Coated Denuders, Cation-Exchange Membranes, and Nylon Membranes: Humidity Influences, Environ. Sci. Technol., 49(10), 6102–6108, doi:10.1021/acs.est.5b00098, 2015.

Huang, J., Miller, M. B., Weiss-Penzias, P. and Gustin, M. S.: Comparison of gaseous oxidized Hg measured by KCl-coated denuders, and nylon and cation exchange membranes, Environmental Science and Technology, 47(13), 7307–7316, 2013.

Hynes, A. J., Donohoue, D. L., Goodsite, M. E. and Hedgecock, I. M.: Our current understanding of major chemical and physical processes affecting mercury dynamics in the atmosphere and at the air-water/terrestrial interfaces, Mercury Fate and Transport in the Global Atmosphere: Emissions, Measurements and Models, (Journal Article), 427–457, 2009.

Jaffe, D. A., Lyman, S., Amos, H. M., Gustin, M. S., Huang, J., Selin, N. E., Levin, L., ter Schure, A., Mason, R. P., Talbot, R., Rutter, A., Finley, B., Jaeglé, L., Shah, V., McClure, C., Ambrose, J., Gratz, L., Lindberg, S., Weiss-Penzias, P., Sheu, G.-R., Feddersen, D., Horvat, M., Dastoor, A.,

Hynes, A. J., Mao, H., Sonke, J. E., Slemr, F., Fisher, J. A., Ebinghaus, R., Zhang, Y. and Edwards, G.: Progress on Understanding Atmospheric Mercury Hampered by Uncertain Measurements, Environ. Sci. Technol., 48(13), 7204–7206, doi:10.1021/es5026432, 2014.

Lyman, S. N., Jaffe, D. A. and Gustin, M. S.: Release of mercury halides from KCl denuders in the presence of ozone, Atmos. Chem. Phys., 10(17), 8197–8204, doi:10.5194/acp-10-8197-2010, 2010.

Mao, H. and Talbot, R.: Speciated mercury at marine, coastal, and inland sites in New England-Part 1: Temporal variability, Atmospheric Chemistry and Physics, 12(11), 5099–5112, 2012.

Mao, H., Talbot, R., Nielsen, C. and Sive, B.: Controls on methanol and acetone in marine and continental atmospheres, Geophys. Res. Lett., 33(2), L02803, doi:10.1029/2005GL024810, 2006.

McClure, C. D., Jaffe, D. A. and Edgerton, E. S.: Evaluation of the KCl Denuder Method for Gaseous Oxidized Mercury using HgBr2 at an In-Service AMNet Site, Environ. Sci. Technol., 48(19), 11437–11444, doi:10.1021/es502545k, 2014.

Pal, B. and Ariya, P. A.: Studies of ozone initiated reactions of gaseous mercury: Kinetics, product studies, and atmospheric implications, Physical Chemistry Chemical Physics, 6(3), 572–579, 2004.

Saiz-Lopez, A., Shillito, J. A., Coe, H., and Plane, J. M. C.: Measurements and modelling of I_2, IO, OIO, BrO and NO_3 in the mid-latitude marine boundary layer, Atmos. Chem. Phys., 6, 1513–1528, doi:10.5194/acp-6-1513-2006, 2006.

Schroeder, W. H. and Munthe, J.: Atmospheric mercury - An overview, Atmospheric Environment, 32(5), 809–822, 1998.

Seigneur, C., Wrobel, J. and Constantinou, E.: A chemical kinetic mechanism for atmospheric inorganic mercury, Environmental Science and Technology, 28(9), 1589–1597, 1994.

Sigler, J. M., Mao, H. and Talbot, R.: Gaseous elemental and reactive mercury in Southern New Hampshire, Atmos. Chem. Phys., 9(6), 1929–1942, doi:10.5194/acp-9-1929-2009, 2009.

Snider, G., Raofie, F. and Ariya, P. A.: Effects of relative humidity and CO(g) on the O_3-initiated oxidation reaction of Hg^0(g): Kinetic & product studies, Physical Chemistry Chemical Physics, 10(36), 5616–5623, 2008.

Spicer, C. W., Satola, J., Abbgy, A. A., Plastridge, R. A. and Cowen, K. A.: Kinetics of Gas-Phase Elemental Mercury Reaction with Halogen Species, Ozone, and Nitrate Radical under Atmospheric Conditions, (Journal Article), 2002.

Subir, M., Ariya, P. A. and Dastoor, A. P.: A review of uncertainties in atmospheric modeling of mercury chemistry I. Uncertainties in existing kinetic parameters - Fundamental limitations and the importance of heterogeneous chemistry, Atmos.Environ., 45(32), 5664–5676, 2011.

Sumner, A. L., Spicer, C. W., Landis, M. S. and Stevens, R. K.: Kinetics of gaseous elemental mercury oxidation reactions under conditions of relevance to the atmosphere, Atmos.Environ., 2011.

Wang, F., Saiz-Lopez, A., Mahajan, A. S., Martín, J. C. G., Armstrong, D., Lemes, M., Hay, T. and Prados-Roman, C.: Enhanced production of oxidised mercury over the tropical Pacific Ocean: A key missing oxidation pathway, Atmospheric Chemistry and Physics, 14(3), 1323–1335, 2014.

Response to anonymous Referee #3

This paper uses a box model to study the controlling processes of GEM oxidation (or GOM formation) at different types of surface sites, and provides new and important information on the chemistry mechanisms of mercury that might occur in the real atmosphere. It fits well into the scope of ACP. I recommend the paper for publication after addressing the following comments.

We thank the reviewer for their thoughtful, constructive comments and suggestions. The manuscript has been revised carefully. Below we addressed the reviews point by point.

A major comment is that the box model simulation results should be compared against the measurements of PBM mixing ratios at these sites. This would help the interpretation of some controlling processes such as gas-particle partitioning in the model.

It is true that high quality GOM and PBM measurements would be of great help for modelling studies to evaluate the schemes such as gas-particle partitioning process as well as to constrain the aqueous reduction rate. However, the inlet of the Tekran speciation sampling system had an elutriator inlet with an acceleration jet to remove aerosols > 2.5 μm so that only fine PBM was measured. The PBM calculated from the box model does not include size fractionation, thus Tekran $PBM_{2.5}$ measurements could not be used to constrain our simulations and further constrain the reduction rate.

Another general comment is that a more detailed description of the box model set up should be given in the paper, for example the exchange of GOM between the free troposphere and the boundary layer. A schematic can be very helpful for the readers to understand which processes are discussed in the model.

We did not include a scheme to account for GOM exchange between the free troposphere and the boundary layer. Such exchange processes are highly parameterized, and location and time dependent. Including such processes could induce another major uncertainty in the model. In this study, we selected clear-sky and calm wind conditions, usually accompanied by strong stability with a strong inversion layer at the top of the daytime convective PBL layer based on measurements from the literature (e.g.Hogan et al., 2009). Minimal entrainment at the top of the boundary layer was thus expected.

Relevant change in revised manuscript: lines 126-128.

The third general comment is that the paper discusses the importance of different oxidized mercury forms through their oxidation pathways. I suggest the authors also discuss the stability of these oxidized forms in the real atmosphere in the particular environment of each site.

This is a valid point. However, since properties of the oxidized forms remain largely unknown, we added a general discussion on the possible impact of different environments on speciation. The discussion added in the text is as follows in section 1 of revised manuscript:

"GOM concentrations and speciation could be impacted by meteorological conditions and chemical conditions in different environments. High solubility of GOM species, possible phase partitioning of HgO as discussed above could all be the reasons causing varying GOM speciation at different locations. For instance, the aerosol type, size distribution, and chemical composition varied largely between the MBL site and inland sites, which may lead to different gas-particle partitioning rates of GOM species."

Relevant change in revised manuscript: lines 90-95.

Specific comments: 1. throughout the paper: the use of the word "case" in this paper may confuse its readers, as it refers to both different observational days and different model simulations. For example, in page 9, section 2.2 "Case selection", and in page 13, section 3.3 "Sensitivity analysis".

We have changed the word "case" in sensitivity studies to "scenario".

Relevant change in revised manuscript: line 368, 370; and all "case" words in section 3.4 were changed to "scenario"; Table 3.

2. Title: it would be better if the full expression of GEM (i.e. gaseous elemental mercury) is given in the title.

Upon the reviewer's suggestion the title was changed to "Investigation of processes controlling summertime gaseous elemental mercury oxidation at mid-latitudinal marine, coastal, and inland sites".

Relevant change in revised manuscript: line 1.

3. Page 4, line 25. Can the authors describe which parameter is used to account for entrainment from the free troposphere?

As we responded above to a comment similar to this, we did not include a scheme to account for GOM exchange between the free troposphere and the boundary layer. Such exchange processes are highly parameterized, and location and time dependent. Including such processes could induce another major uncertainty in the model. In this study, we selected clear-sky and calm wind conditions, usually accompanied by strong stability with a strong inversion layer at the top of the daytime convective PBL layer based on measurements from the literature (e.g., Hogan et al., 2009). Minimal entrainment at the top of the boundary layer was thus expected.

Relevant change in revised manuscript: lines 126-128.

4. Page 5, line 12. I do not understand why the "GEM mixing ratios ... are set to be constant mimicking GEM emission flux". What does this mean in the model?

Revised to "the initial GEM mixing ratios along with a list of compounds (Table 2) in the model were obtained from observations in three different environments are were set to be constant during simulations". The theory behind the fixed input concentrations of GEM among a number of other compounds is that a box model simulates the concentrations of short-lived compounds reaching an instantaneous chemical steady state, and for the time scales of such instants, the chemicals such as GEM are long-lived enough to maintain a constant level. We have added this explanation in the text.

Relevant change in revised manuscript: lines 130-136.

5. Page 6, line 8. The numbers of reactions are incorrect.

Corrected.

Relevant change in revised manuscript: line 161.

6. Page 6, lines 11-18. The reaction constants for these aqueous Hg reactions should be given either in the main text or in the supplement. Also, I speculate these reactions are also highly uncertain. Do the authors consider the uncertainties associated with them?

A table showing aqueous Hg reactions in our model was added as Table S1.

Aqueous Hg reduction is one of the major sources of GEM in the atmosphere. Therefore, aqueous Hg reactions is supposed to be a factor controlling GEM mixing ratios, which turns out to influence GOM mixing ratios. However, aqueous Hg reduction is not an important control on GOM simulations in this study because GEM mixing ratios in the model were fixed using observed values. The uncertainties associated with aqueous Hg reactions would not influence GEM mixing ratios and therefore have minor effects on simulated GOM mixing ratios.

Relevant change in revised manuscript: Table S1 was added.

7. Page 12, lines 1-9. These several sentences are confusing. At first, it is mentioned that "the patterns of diurnal variation were similar at the three sites". Then, it is said that "PM showed negligible diurnal variation". I suggest that a statistical method is used to quantitatively detect the diurnal patterns at all the sites.

We apologize for the confusion. All three sites did show diurnal cycles, the expression of "PM showed negligible diurnal variation" were intended to suggest the daily amplitude is very small compared to that at AI and TF. We have rephrased these sentences to clarify the point. The changed wording is as follows:

"The patterns of diurnal variation were similar at the three sites with small discrepancy on the occurring time of daily peaks (~ 13:00 LT at AI, and ~14:00 LT at TF and PM), but the magnitude varied largely by site. AI had the largest GOM diurnal amplitude (i.e., daily maximum – daily minimum) ranging from 0.73 to 13.29 ppqv, TF from 0.05 to 0.57 ppqv, and PM showed a very small range from 0.05 to 0.14 ppqv."

Relevant change in revised manuscript: lines 299-303.

8. Table 2: How uncertain are the simulated [Br] at TF and PM? What is the major source of [Br]? How is the concentration of Br_2 set in the box model? In addition, are the boundary layer heights at AI and PM set to be constant? Do the authors expect any diurnal variations of the boundary layer height?

No observations of [Br] were available at the three sites. At AI, we used [BrO] observation from Saiz-Lopez et al. (2006) to constrain simulated [BrO]. However, at TF and PM, we don't have any data available to constrain Br species, so we did not give a specific source for Br and BrO. [Br_2] initial concentration was set to 1 pptv (e.g. Finley et al., 2008) but without setting it as constant. In result, Br_2 was rapidly depleted during daytime simulations with very low concentration of Br and BrO produced. Average daytime maximum of [BrO] is about 10 ppqv, and [Br] is negligible. The model simulation at TF and PM indicated that O_3 and OH were sufficient for GOM production at TF and PM.

The boundary layer heights at AI and PM were set to be constant. The major reason is we do not have diurnal cycle data of boundary layer height at AI and PM. Moreover, in the MBL, boundary layer height is usually a few hundred meters and does not vary much (Vickers and Mahrt, 2003; Angevine et al., 2006). At PM, the boundary layer height is set as averaged daytime boundary height at TF minus the elevation difference between the two sites. At night, due to its high elevation, it was above the nocturnal boundary layer.

Relevant change in revised manuscript: lines 203-207.

9. Figures: The figures throughout the paper should use a consistent way of uncertainty quantification, probably being consistent with the statistical method used for the observations

(Figure 1). In the current paper, min-max, standard deviation, and box-whiskers all exist making the readers difficult to compare the uncertainties among these figures.

We revised the figures and used error bars for standard deviation only.

Relevant change in revised manuscript: Figure 2, Figure 4, Figure 6, and Figure 8.

In addition, I suggest the authors merge Figures 2, 3, and 8.

Thank you for the suggestion. We merged these three figures to Figure 2 in the revised manuscript. The merged figure was shown below (Fig. 1):

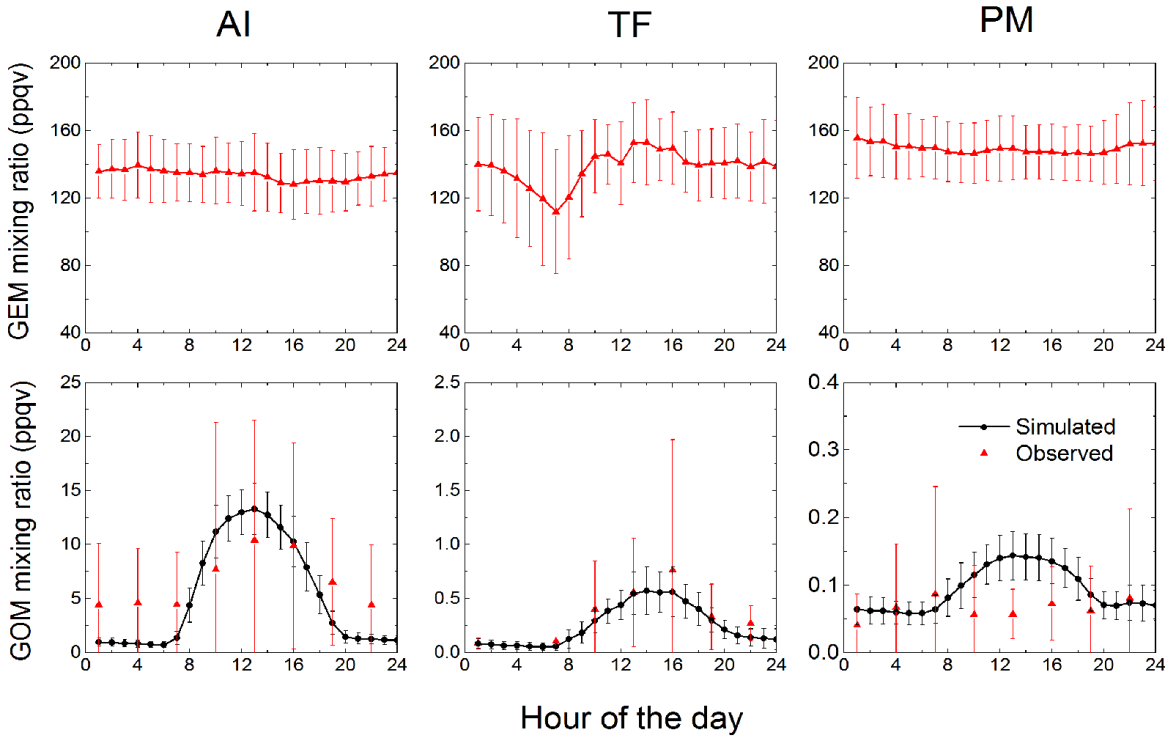

Figure 1. Average diurnal cycles of observed GEM (top panel) and simulated and observed GOM (bottom panel) averaged over the selected 50 days at Appledore Island (AI), 12 days at Thompson Farm (TF), and 21 days at Pack Monadnock (PM) from summers of 2007, 2008, and 2010. The error bars represent standard deviation.

Relevant change in revised manuscript: Figure 2.

References

Angevine, W. M., Hare, J. E., Fairall, C. W., Wolfe, D. E., Hill, R. J., Brewer, W. A. and White, A. B.: Structure and formation of the highly stable marine boundary layer over the Gulf of Maine, J. Geophys. Res., 111(D23), D23S22, doi:10.1029/2006JD007465, 2006.

Finley, B. D. and Saltzman, E. S.: Observations of Cl_2, Br_2, and I_2 in coastal marine air, J. Geophys. Res., 113(D21), D21301, doi:10.1029/2008JD010269, 2008.

Hogan, R. J., Grant, A. L. M., Illingworth, A. J., Pearson, G. N. and O'Connor, E. J.: Vertical velocity variance and skewness in clear and cloud-topped boundary layers as revealed by Doppler lidar, Q.J.R. Meteorol. Soc., 135(640), 635–643, doi:10.1002/qj.413, 2009.

Saiz-Lopez, A., Shillito, J. A., Coe, H., and Plane, J. M. C.: Measurements and modelling of I_2, IO, OIO, BrO and NO_3 in the mid-latitude marine boundary layer, Atmos. Chem. Phys., 6, 1513–1528, doi:10.5194/acp-6-1513-2006, 2006.

Vickers, D. and Mahrt, L.: Evaluating Formulations of Stable Boundary Layer Height, doi:10.1175/JAM2160.1, 2004.

Investigation of processes controlling summertime gaseous elemental mercury ~~GEM~~ oxidation at mid-latitudinal marine, coastal, and inland Sites

Z. Ye[1], H. Mao[1], C.-J. Lin[2,3], and S. Y. Kim[4]

[1] Department of Chemistry, State University of New York College of Environmental Science and Forestry, Syracuse, NY, 13210, USA

[2] Center for Advances in Water and Air Quality, Lamar University, Beaumont, TX, 77710, USA

[3] Department of Civil and Environmental Engineering, Lamar University, Beaumont, TX, 77710, USA

[4] R&D Program Evaluation Division Office of National Evaluation and Analysis Korea Institute of S&T Evaluation and Planning (KISTEP), Seoul, South Korea

Received: 13 October 2015 – Accepted: 23 October 2015 – Published: 15 January 2016

Correspondence to: Z. Ye (zye01@syr.edu)

Abstract

A box model incorporating a state-of-the-art chemical mechanism for atmospheric mercury (Hg) cycling was developed to investigate oxidation of gaseous elemental mercury (GEM) at three locations in the northeastern United States: Appledore Island (marine), Thompson Farm (coastal, rural), and Pack Monadnock (inland, rural, elevated). The chemical mechanism in this box model included the most up-to-date Hg and halogen chemistry. As a result, the box model was able to simulate reasonably the observed diurnal cycles of gaseous oxidized mercury (GOM) and chemical speciation bearing distinct differences between the three sites. In agreement with observations, simulated GOM diurnal cycles at AI and TF showed significant daytime peaks in the afternoon and nighttime minimums compared to flat GOM diurnal cycles at PM. Moreover, and significant differences in magnitude of GOM diurnal amplitude (AI>TF>PM) were captured in modeled results. ~~The chemical mechanism improved model's ability to simulate the formation of gaseous oxidized mercury (GOM) at the study sites.~~ At the coastal and inland sites, GEM oxidation was predominated by O_3 and OH, contributing 80–99% of total GOM production during daytime. H_2O_2 initiated GEM oxidation was significant (~33% of the total GOM) at the inland site during nighttime. In the marine boundary layer (MBL)~~,~~ atmosphere, Br and BrO became ~~were~~ dominant GEM oxidants with mixing ratios reaching 0.1 and 1 pptv, respectively, contributing ~70% of the total GOM production during mid-day, while O_3 dominated GEM oxidation (50–90% of GOM production) over the remaining day when Br and BrO mixing ratios were diminished. ~~Following the production of HgBr from GEM+Br, t~~The majority of HgBr produced from GEM+Br was oxidized by NO_2 and HO_2 ~~BrO, HO_2, OH, ClO, and IO~~ to form ~~Hg(II)~~ brominated GOM species. ~~However, under atmospheric conditions, the prevalent GEM oxidants in the MBL could be Br /BrO or O_3 /OH depending on Br and BrO mixing ratios.~~ Relative humidity and products of the

CH_3O_2+BrO reaction possibly affected significantly the mixing ratios of Br or BrO radicals and subsequently GOM formation. Gas-particle partitioning could be potentially important in the production of GOM as well as Br and BrO at the marine site.

1 Introduction

Mercury (Hg) is a toxic pollutant found globally in air, natural waters, and soils. The health concern of Hg arises from the neurotoxic organic form, methyl mercury (MeHg), in the aquatic environments (Mason et al., 2006; Miller et al., 2007; Rolfhus et al., 2003). The high bioaccumulation and biomagnification of MeHg lead to human exposure through the consumption of seafood (Clarkson, 1994). Deposition of atmospheric Hg is one of the most important sources of aquatic Hg.

In the atmosphere, Hg exists in three forms: gaseous elemental mercury (GEM), gaseous oxidized mercury (GOM), and particulate bound mercury (PBM). The majority of atmospheric Hg is GEM, comprising > 95% of total gaseous mercury (TGM=GEM+GOM). The 0.8–1.7 years atmospheric lifetime of GEM is conducive to long range transport of Hg as a global pollutant (Bergan et al., 1999; Bergan and Rodhe, 2001; Holmes et al., 2006; Lin and Pehkonen, 1999; Schroeder and Munthe, 1998; Selin et al., 2007). In contrast, GOM and PBM are relatively short-lived and subject to ~~dry and~~ wet deposition and stronger dry deposition than GEM due to their high solubility in water and low vapor pressure. GOM in the atmosphere can be produced from oxidation of GEM, released directly from anthropogenic emissions, and transformed from PBM. In remote regions, in-situ GOM production may be the major source of GOM (Weiss-Penzias et al., 2003; Poissant et al., 2004; Mao and Talbot, 2012) considering its short lifetime. ~~Oxidation of GEM was usually thought to be a major source of GOM in remote regions.~~

Chemical speciation of atmospheric Hg is essential to understand its geochemical cycle. Theoretical and experimental studies suggested that the main oxidants of GEM in the atmosphere are ozone (O_3), hydroxyl radical (OH), atomic bromine (Br), bromine monoxide (BrO), hydrogen peroxide (H_2O_2), and atomic chlorine (Cl), yielding GOM species of HgO, HgBrO, HgBr,

63 $Hg(OH)_2$, HgCl, and through further reaction to other mercury halides (Ariya et al., 2015; Dibble
64 et al., 2012; Lin and Pehkonen, 1999). Although efforts have been made to investigate the relative
65 importance of these oxidants for GEM oxidation in the troposphere, it is still not well understood.
66 In the terrestrial environment, it was suggested that the oxidation of GEM was primarily by O_3 and
67 OH radicals (Shon et al., 2005; Sillman et al., 2007). The speciation and quantification of GEM +
68 O_3 product(s) still remain unknown and debatable (Ariya et al., 2015; Gustin et al., 2013; Rutter
69 et al., 2012). An experimental study by Pal and Ariya (2004b) measured 1% of HgO produced by
70 GEM + O_3 on an aerosol filter. Snider et al. (2008) showed HgO(s) production in their kinetic and
71 product study. Schroeder et al. (1998) suggested HgO would not exist as an isolated molecule in
72 gas phase but could be deposited to and retained by manifold given a decomposition temperature
73 of +500 °C. However, the GEM + O_3 reaction and decomposition temperature (Schroeder et al.,
74 1998) could also be impacted by the presence of other ambient gases (Snider et al., 2008; Gustin
75 et al., 2013; Seigneur et al., 1994). A recent study of Huang et al. (2013) observed gas-phase HgO
76 using nylon and cation exchange membranes. ~~In recent years, a consensus has emerged that the~~
77 ~~GEM+O_3 reaction most likely occurs with solid phase products, whose speciation and~~
78 ~~quantification remain unknown (Ariya et al., 2015; Pal and Ariya, 2004b; Rutter et al., 2012;~~
79 ~~Snider et al., 2008).~~ The reaction of GEM+OH has been subject to debate between theoretical and
80 experimental studies, as no mechanism ~~that is~~ consistent with thermochemistry has been proposed
81 (Ariya et al., 2015; Pal and Ariya, 2004a; Subir et al., 2011). ~~In the MBL, m~~Measurement~~s of~~
82 ~~GOM in~~ studies on GOM in ~~the~~ polar regions (Simpson et al., 2007; Steffen et al., 2008) ~~to~~ and
83 sub-tropical MBL (Laurier et al., 2003; Laurier and Mason, 2007; Obrist et al., 2011) ~~and~~ as well
84 as atmospheric modeling studies on mercury ~~models~~ cycling (Holmes et al., 2009, 2010; Kim et
85 al., 2010; Lindberg et al., 2002; Obrist et al., 2011; Soerensen et al., 2010; Toyota et al., 2014;

Wang et al., 2014; Xie et al., 2008) have ~~also~~ suggested Br as an important oxidant of GEM. The major source of atmospheric Br was suggested to be produced photolytically from Br-containing compounds and through the Br/BrO cycle involving tropospheric O_3 (Saiz-Lopez and Glasow, 2012; Simpson et al., 2015).

GOM concentrations and speciation could be impacted by meteorological conditions and chemical conditions in different environments. High solubility of GOM species, possible phase partitioning of HgO as discussed above could all be the reasons causing varying GOM speciation at different locations. For instance, the aerosol type, size distribution, and chemical composition varied largely between the MBL site and inland sites, which may lead to different gas-particle partitioning rates of GOM species.

Hg chemistry in the MBL, the lowest part of the troposphere in direct contact with the sea surface, has global importance as approximately 70% of the earth's surface is covered by oceans (Glasow et al., 2002). Hg in the MBL cycles differently from in coastal or inland areas. However, contemporary models are not able to reproduce GOM observations temporally and spatially due to knowledge gaps in Hg science, simplified model assumptions, and uncertainties of measurements (Ariya et al., 2015; Lin et al., 2006). In the polar region, bromine radicals were identified as the primary cause of the Arctic mercury depletion events (AMDE) (Kim et al., 2010; Lindberg et al., 2002; Toyota et al., 2014; Xie et al., 2008). In the MBL outside Polar Regions, due to lower mixing ratios of atmospheric halogen radicals, often lower than the detection limit, mechanisms for GOM production were more controversial than in ~~the~~ Polar Regions. Using a box model, Hedgecock et al. (Hedgecock et al., 2003; Hedgecock and Pirrone, 2004, 2005) suggested that O_3 was a dominant GEM oxidant in the MBL at mid-latitudes in the Mediterranean region, and that the GEM+O_3 reaction may form solid products. However, the reaction kinetics in their

model were out-of-date with limited halogen chemistry, and fixed emissions used in the model oversimplified the source terms. Holmes et al. (2009) simulated that GEM oxidation by Br comprised 35–60% of the GOM sources using BrO concentrations calculated at a photostationary state from a prescribed distribution of Br mixing ratios. Additionally, ~~In this study~~ a parameter was introduced in the same study to account for entrainment of free tropospheric GOM into the MBL and the Br mixing ratio was adjusted to capture the observed GOM diurnal trend, which could cause large uncertainties in GOM simulations. Most recently, Wang et al. (2014) employed updated Hg reactions together with bromine and iodine reactions, adopting the free tropospheric GOM entrainment parameter from Holmes et al. (2009) for tropical MBL, and found Br to be a primary GEM oxidant, but oxidation by Br or O_3/OH alone was unable to reproduce observed GOM concentration. However, different GEM oxidants could be dominant in different environments, as a result of the unique composition and concentration levels of in-situ oxidants those environments may be characterized with.

In this study, we employed a state-of-the-art chemical mechanism that incorporates gas and aqueous phase chemistry of Hg, O_3, and halogen to investigate the dynamics of GOM formation under various atmospheric conditions in mid-latitude regions. The most up-to-date kinetics was applied. Halogen radical mixing ratios (such as Br and BrO) were calculated using up-to-date atmospheric halogen reactions. Clear sky days with calm wind conditions were selected, which are mostly associated with strong atmospheric stability, to minimize the entrainment effect of free tropospheric air and regional transport and hence no entrainment factor was included in this study. Moreover, the initial GEM mixing ratios along with a list of compounds (Table 2) in the model were obtained from observations in three different environments and were set to be constant during simulations~~mimicking GEM emission flux~~. Fixing the input concentrations of GEM among a

number of other compounds (Table 2) as constants using observational data enabled a modeled chemical environment close to the real atmospheric environment that is being studied. Moreover, a box model simulates the concentrations of short-lived compounds reaching an instantaneous chemical steady state, and for the time scales of such instants, the chemicals such as GEM are long-lived enough to maintain a constant level. In Section 2, the methods employed were laid out in detail. Section 3 presented results of reasonably simulated differences between GOM diurnal cycles at the three locations that were captured in measurement data, major GEM oxidants in the three environments, and a detailed discussion of the sensitivity of physical parameters and important chemical reactions. Section 4 summarized the key findings and implications from this study.

2 Methods

2.1 Box Model Description

The Kinetic PreProcessor version 2.1 (Sandu and Sander, 2006) was utilized as the framework of the box model (Hedgecock et al., 2003; Hedgecock and Pirrone, 2004, 2005). A second order Rosenbrock method (Verwer et al., 1999) was applied to solve the coupled ordinary differential equations. The box model used in this study was initially set up by Kim et al. (2010). It was further improved in this study by incorporating the most up-to-date gas and aqueous phase chemical mechanisms (Atkinson et al., 2004, 2008; Dibble et al., 2012; Sander et al., 2011) to the model.

2.1.1 Reactions and kinetics

The box model has a total of 424 reactions: 276 gas-phase reactions (including Hg, halogen, O_3, sulfate, and hydrocarbon reactions), 52 gas-water equilibriums, 28 aqueous equilibriums and 68 aqueous reactions. Most of these reactions and kinetic data were updated based on JPL Report

No. 17 (Sander et al., 2011), the halogen chemistry reviews of Atkinson et al. (2004, 2008), and the references listed in Table 1. Photodissociation coefficients were calculated from the Tropospheric Ultraviolet and Visible (TUV) Radiation Model (Madronich, 1993).

The most important improvements in chemistry are gas and aerosol phase of Hg and halogen reactions. Gas-phase Hg reactions included in the box model are (Table 1):

1. Oxidation of GEM by O_3, OH, H_2O_2, Br, BrO, Cl, Cl_2, I (G1–8);

2. Reduction of HgBr and HgI to produce GEM (G9–11); and

3. Reactions of HgBr/HgCl with BrO, ClO, IO, NO_2, HO_2, and OH (G12–24) with kinetics suggested by Dibble et al. (2012).

Aqueous Hg reactions include (Table S1):

1. Oxidations of Hg by O_3, OH, HOCl, and ClO^-, further oxidation of HgOH by O_2;

2. Reduction of Hg^{2+} by HO_2, photolytic reduction of $Hg(OH)_2$ and S(IV)-mediated reduction; and

3. Aqueous equilibria involving $HgSO_3$, $Hg(SO_3)_2^{2-}$, $HgOH^+$ and $Hg(OH)_2$. Gasphase halogen reactions in the box model are mainly cycles of halogen radicals (Cl/Br/I and ClO/BrO/IO radicals).

The Cl/Br/I radical cycles include photodissociation of Cl_2/Br_2/I_2, organic halides, and other inorganic halides as sources, and oxidation reactions as sinks. The ClO/BrO/IO radical cycles involve oxidation of Cl/Br/I radicals, photodissociation of $ClNO_2$/$ClONO_2$/$BrNO_2$/$BrONO_2$, production from other halogen radicals, and sink reactions to ~~reproduce~~ calculate Cl/Br/I~~O~~ radicals or other halides. Aqueous halogen reactions include reactions of Br^-/Cl^- and reactions of aqueous BrCl, HCl, HBr, HOCl, HOBr, Cl_2, and Br_2 species. The chemistry of halogen radicals, especially the reaction cycles of Br and BrO radicals, could be important and should not be neglected or

replaced by simple approximation ~~as previous Hg box model studies outside of Polar regions did~~. Hence, the most up-to-date halogen chemistry from the literature was included in our model.

2.1.2 Initial conditions and input data

Observations at three sites from the University of New Hampshire (UNH) AIRMAP Observing Network (http://www.eos.unh.edu/observatories/data.shtml) were used: a marine site located on Appledore Island (AI) at the Shoals Marine Lab, ~~in~~ the Gulf of Maine (42.97°N, 70.62°W, 40 m a.s.l.), a coastal site located in Thompson Farm (TF) in Durham, NH (43.11°N, 70.95°W, 24 m a.s.l.) and 25 km away from the Gulf of Maine ~~(43.11°N, 70.95°W, 24 m a.s.l.)~~, and a~~n~~ forested 90 km inland site located on Pack Monadnock (PM) in Miller State Park in Peterborough, NH (42.86°N, 71.88°W, 700 m a.s.l.) (Fig. 1). Hourly mean values of GEM, O_3, CO, NO, meteorological observations (i.e., temperature, relative humidity, ~~wind speed,~~ and solar radiation) at these three sites were used as initial input to the box model. For species that were not measured, we set their initial concentrations as the values in similar environments from the literature if available. Observations of GOM mixing ratios from the three sites were utilized to evaluate the model performance. GEM and GOM data were collected using the Tekran® 2537/1130/1135 speciation unit (Tekran Inc., Canada). For these three sites, the instruments were first run and calibrated in the laboratory and then operated at the sites in a consistent manner. GEM was measured at 5-min intervals and with a limit of detection (LOD) of ~5-10 ppqv (Mao et al., 2008), GOM was measured over a 2-h sampling period with a LOD of ~0.1 ppqv based on three times the standard deviation of the field blank values (Sigler et al., 2009; Mao and Talbot, 2012). A custom-built refrigerator assembly and a canister of drierite was used to cool and dry air streams before entering into the 1130 pump module, resulting in < 25% RH of air streams (Sigler et al., 2009). Detailed information on these measurements can be found in Mao and Talbot (2004; 2012),

Talbot et al. (2005), Fischer et al. (2007), Mao et al. (2008), and Sigler et al. (2009). Table 2 lists the input variables of the box model. The model's initial mixing ratios of GEM, O_3, CO, and NO were obtained from observations and were set to be constant during ~~a~~each 1h simulation. Br/Cl/I concentrations were all calculated from the model given initial concentrations of 1 pptv (Finley et al., 2008; except for AI) for Br_2, Cl_2, and I_2 species. At AI, the Br_2 initial concentration was set to be constant during simulations and used Saiz-Lopez et al. (2006)'s values to constrain [BrO]. Detailed information can be found in Section 3.3.1. Dry deposition flux was calculated using dry deposition velocity data derived from Zhang et al. (2009, 2012) and boundary layer height estimated from Mao and Talbot (2004). Other physical parameters (i.e. Henry's constants, liquid water content, and aerosol radius) were used to simulate the gas-particle partitioning process in the box model.

2.1.3 Gas-particle partitioning

An empirical expression was utilized to calculate particle size growth relative to its dry radius (r_{dry}) (Lewis and Schwartz, 2006):

$$r = r_{dry} \frac{4}{3.7} \left(\frac{2-RH}{1-RH}\right)^{1/3}, \quad (1)$$

where RH is the relative humidity, and r is the particle radius at RH.

Gas-particle partitioning was treated by mass transfer between droplets and air. The dynamic mass transfer coefficient across the gas-aqueous interface was calculated using the method developed by Schwartz (1986). The net mass flux (F, molecule cm^{-3} s^{-1}) between the gas and aqueous phase is given by

$$F = k_{mt} \times (L \times c_g - \frac{c_{aq}}{HRT}), \quad (2)$$

where L is the liquid water content ($m^3_{water} m^{-3}_{air}$), k_{mt} is the mass transfer coefficient (s^{-1}), c_g is the gas phase concentration of the species (molecules cm^{-3}), c_{aq} is the aqueous phase concentration of

species (molecules cm^{-3}), H is the Henry's constant of the species (M atm^{-1}), R is the universal gas constant (atm L K^{-1} mol^{-1}), and T is atmospheric temperature (K). k_{mt} is calculated as follow:

$$k_{mt} = \left(\frac{r^2}{3D_g} + \frac{4r}{3\bar{v}\alpha}\right)^{-1}, \quad (3)$$

$$\bar{v} = (8RT/M\pi)^{1/2}, \quad (4)$$

where r is the particle radius (μm), D_g is the diffusion coefficient ($m^2 s^{-1}$), $\bar{v}$ is the mean thermal molecular velocity (m s^{-1}), α is the dimensionless accommodation coefficient, and M is the species molecular weight (g mol^{-1}).

2.2 Case Selection

A total of 83 cases were examined to investigate the role of chemistry in Hg cycling in the MBL, coastal, and inland environments. At the study sites, significant warm season declines of GEM were observed with annual maximums in spring and minimums in autumn resulting in seasonal amplitudes up to 100 ppqv at TF (Mao et al., 2008). The lost GEM during the warm season most likely entered the ecosystem. Chemical transformation of GEM in warm seasons was suspected to be one of the factors causing the observed seasonal decline in GEM. As such, this study selected the cases representing summer days when chemical processes were most likely dominant. To exclude the influence of wet deposition, we selected clear-sky conditions based on the observed photodissociation rate constant of NO_2 (jNO_2) and solar radiation flux. To minimize the influence of transport, cases with arithmetic daily mean wind speed higher than 75% percentile of all summer days in studied years (> 1.3 m s^{-1} at TF, > 6 m s^{-1} at PM, and > 7 m s^{-1} at AI) were excluded. As a result, 50, 12, and 21 clear-sky days at AI (marine), TF (coastal), and PM (inland, elevated), respectively, were selected from summers of 2007, 2008, and 2010. Since there was no temperature data available for summer 2009 at TF, 2009 was not considered.

2.3 Backward Trajectory Model

The National Oceanic and Atmospheric Administration (NOAA) Hybrid Single Particle Lagrangian Integrated Trajectory (HYSPLIT) trajectory model was used to identify source regions of air masses at the three sites. The model runs were performed over twenty-four hours using the NOAA NAM (Eta) Data Assimilation System (EDAS) data with a 40km×40km horizontal resolution as input. Backward trajectories and trajectory clusters were calculated.

2.4 Model Evaluation

To evaluate the box model performance with observations, the following statistical performance measures (Chang and Hanna, 2004; Hanna, 1988; Hanna et al., 1991, 1993), which include the ~~functional~~ fractional bias (FB), the normalized mean square error (NMSE), the root mean square error (RMSE), and the partition of NMSE due to systematic errors ($NMSE_s$) were used:

$$FB = \left(\overline{C_0} - \overline{C_p}\right)/0.5\left(\overline{C_0} + \overline{C_p}\right), \quad (5)$$

$$NMSE = \overline{\left(C_0 - C_p\right)^2}/\overline{C_0}\,\overline{C_p}, \quad (6)$$

$$RMSE = \sqrt{\overline{\left(C_0 - C_p\right)^2}}, \quad (7)$$

$$NMSE_s = 4FB^2/(4 - FB^2), \quad (8)$$

where C_p is model predictions, C_0 is observations, overbar ($\bar{C}$) is average over the dataset.

3 Results and Discussion

3.1 General characteristics in measured GOM and GEM

In the selected 83 cases, atmospheric GOM and GEM mixing ratios varied greatly at the three sites (Fig. 2). Mixing ratios of GOM varied over 0.03–87.79 ppqv at AI, 0.04–4.93 ppqv at TF, and 0–0.65 ppqv at PM. ~~GOM did not show consistent diurnal variation at these sites.~~ At AI

and TF, significant diurnal variation was observed with afternoon maximums and nighttime minimums. At AI, GOM peaked at 10 ppqv over 14:00–16:00 EDT and was ~ 5 ppqv at night, well above the ~~limit of detection~~LOD (~~LOD,~~ ~ 0.1 ppqv, from Sigler et al., 2009, the same LOD for the instruments at the three sites). At TF, GOM mixing ratios peaked at 0.75 ppqv at 17:00 EDT and were below LOD at night, before 08:00 EDT. The GOM diurnal cycle at PM was different from that at AI and TF. At PM, averaged GOM had higher mixing ratios at night and in the early morning than in the afternoon. However, the median values ~~were showing~~ showed afternoon peaks and nighttime minimums. The difference between average and median GOM diurnal cycles was driven by 3 cases that had abnormally high GOM mixing ratios (> 0.6 ppqv) at night or in the early morning relative to the average GOM mixing ratio through the day (~ 0.1 ppqv).

Mixing ratios of GEM ranged over 65–231 ppqv at AI, 60–213 ppqv at TF, and 121– 231 ppqv at PM (Fig. 2). On average, GEM mixing ratios at PM were 8% higher than that at TF and 12% higher than that at AI. Unlike GOM, GEM diurnal cycles showed nearly flat patterns at AI and PM, though slightly higher (~ 3 %) GEM mixing ratios at night than in the daytime were observed at PM. In contrast, the average GEM diurnal cycle at TF showed an early morning (07:00 EDT) minimum (112 ppqv) and a daytime (13:00 EDT) maximum (153 ppqv).

The site differences of GOM and GEM diurnal cycles could be attributed to different chemical environments, land surface types, and meteorological conditions. For example, the GEM daily minimum at night and in the early morning at TF was likely caused by a strong net loss dominated by dry deposition under nocturnal inversion (Mao et al., 2008; Mao and Talbot, 2012). Nocturnal inversion also influenced the GEM and GOM diurnal cycles at PM, albeit differently from at TF. The elevation of PM site is 700ma.s.l., above the nocturnal inversion layer (< 200 m)

(e.g. Kutsher et al., 2012), and thus GEM and GOM at night were continuously replenished by those produced from daytime and remaining in the residual layer, which likely caused higher nighttime values at PM. Daytime peaks of GOM at TF and AI were most likely caused by photochemical oxidation of GEM under strong solar radiation. The causes for such variation were examined in Sect. 3.~~2~~4.2.

3.2 Simulated diurnal variation and speciation of GOM

Model simulated diurnal cycles of GOM averaged over the 50, 12, and 21 clear-sky days at AI, TF, and PM, respectively, were shown in Fig. 2~~3~~. The patterns of diurnal variation were similar at the three sites with small discrepancy on the occurring time of daily peaks ~~at (~~ 1~~3~~4:00 LT at AI, and ~14:00 LT at TF and PM), but the magnitude varied large by site. AI had the largest GOM diurnal amplitude (i.e., daily maximum – daily minimum) ranging from ~~0.45~~ 0.73 to ~~20.99~~13.29 ppqv, TF from 0.0~~5~~2 to ~~1.85~~0.57 ppqv, and PM showed a very small range from 0.05 to 0.14 ppqv ~~showed negligible diurnal variation~~. Similar magnitude variation was also exhibited in GOM observations (Fig. 2). Overall, simulated GOM mixing ratios at the three sites were in agreement with observations (detailed comparison in Sect. 3.~~4~~3).

The simulations suggested that the dominant GOM species and GEM oxidants varied by site (Fig. ~~4~~3). At AI, brominated GOM species comprised 59~~50~~–~~71~~81% of the total GOM over ~~09~~08:00–~~16~~18:00 EDT, whereas HgO was dominant (~~56~~50–92% of the total GOM) during the remaining day. At TF and PM, HgO was the predominant GOM species (~~80~~62–~~99~~88%). HgO was produced from oxidation of GEM by O_3 and OH. The contribution to HgO from oxidation by O_3 was larger than by OH except at noon when OH mixing ratios reach daily peaks resulting in comparable contributions (48 and 52% by OH and O_3, respectively). At AI, $BrHgNO_2$ and HgBrO~~,~~ ~~BrHgOOH, and BrHgOBr~~ were the most abundant brominated GOM species, which constituted ~

~~99~~96% of the total brominated GOM. HgBrO was produced from the GEM + BrO reaction, while ~~BrHgOOH and BrHgOBr~~ $BrHgNO_2$ were produced from GEM oxidation by Br radicals followed by reactions of HgBr with ~~HO_2 and BrO~~ NO_2. $Hg(OH)_2$ from GEM oxidation by H_2O_2 appeared to be an important nighttime GOM species at the inland site (PM), accounting for 33% of the total GOM at night. Other GOM species were negligible in the studied cases.

3.3 Model evaluation

For all cases at AI and TF, the average simulated and observed GOM diurnal cycles agreed reasonably well in both magnitude and shape, whereas at PM the model appeared to have missed both (Fig. ~~8~~2). Three salient features were noted for the disagreement between the model and observational results. First, the standard deviation ~~from of observations~~ observed GOM mixing ratios was a factor of 2–7 larger than that of the simulated. This suggested that the model could capture the mean values of GOM, but not the very low and very large mixing ratios. Second, observed nighttime GOM mixing ratios were 12–200% larger than the simulated at AI, indicating that the model did not capture certain nighttime processes producing GOM in the ~~marine boundary layer~~MBL. Third, the simulated diurnal cycle was the opposite of the observed at PM, with the maximum during the day and minimum at night. It was likely that the model simply simulated the dependence of GOM production on solar radiation. At PM, more processes may have contributed to the diurnal variation. At night, the site is above the nocturnal boundary layer and exposed to the GOM produced in the preceding convective boundary layer~~from the daytime~~, which could continually replenish surface GOM at the site that was lost via dry deposition and perhaps reduction. The model-observation discrepancies of GOM ~~for~~ at the three sites were discussed as follows.

3.3.1 Appledore Island (marine)

Of the 50 cases at AI, 27 diurnal cycles of GOM were simulated with the average values and patterns close to the observed and $NMSE_s$ = ~~2.86~~1.88%, denoted as *matching* cases hereafter, 8 were underestimated with $NMSE_s$ = ~~146~~121%, and 15 were overestimated with $NMSE_s$ = ~~167~~171%. The observed and simulated average GOM mixing ratios and the corresponding ranges were calculated for the matching, under-estimation, and over-estimation cases at AI (Fig. ~~9a~~4a). For more than half of the time (27 matching cases out of 50 cases in total), the model captured the average GOM diurnal cycle, the diurnal cycle pattern and overall GOM levels. Beyond that, Fig. ~~9a~~ 4a shows large difference in the observed GOM levels among the matching, under-estimation, and over-estimation cases. On average, the observed daytime peak in the under-estimation cases was about twice as large as that for the matching cases and 7 times larger than that for the over-estimation cases. However, such difference was not captured by the model, suggesting that ~~one or more~~ some GOM producing processes in the MBL were not included or not realistically represented in the box model. In addition, the GOM diurnal pattern ~~of~~ in the over-estimation cases was different from those in the under-estimation and matching cases. The average observed GOM diurnal cycles of the under-estimation and matching cases both exhibited a daily maximum at 13:00 EDT and a minimum over 04:00–08:00 EDT, whereas ~~for~~ the over-estimation cases showed a daily maximum at around 20:00 EDT and a minimum at 07:00–08:00EDT.

Such differences were due ~~caused~~ possibly to ~~by~~ the challenges of simulating Br and BrO in the MBL at AI. No measurements of Br and BrO radicals as well as Br_2 were available at AI. To reasonably simulate mixing ratios of Br and BrO, Br_2 mixing ratios were calculated based on the BrO observations at a mid-latitude MBL site from Saiz-Lopez et al. (2006), which was ~5.6 ppqv during the daytime (06:00–21:00 EDT). Saiz-Lopez et al. (2006) showed that ~~the~~ daytime

peak mixing ratios of BrO in the MBL could vary by a factor of 2 over a time period of 3 days. Such variation was not captured in our box model, potentially resulting in ~~which could result in~~ uncertainty of up to 100% in simulated Br mixing ratios with subsequent effects on GOM simulation.

In the over-estimation cases, the simulated GOM daytime peaks were very low~~,~~ and appeared later during the day than in the under-estimation and matching cases. Considering the late afternoon peak (17:00 EDT) of O_3 compared to the noontime peak of Br radicals, O_3 possibly played a more important role in the over-estimation cases. To verify this hypothesis, a sensitivity simulation was conducted without the initial Br_2 mixing ratio fixed for these cases, termed as the O_3/OH scenario ~~case~~. In this ~~case~~sensitivity runs, the Br_2 concentration rapidly diminished with time ~~and consequently~~leading to very low ~~the~~ concentrations of Br and BrO ~~were very low~~. The O_3/OH scenario ~~case~~ turned out to better represent these 15 overestimation cases with $NMSE_s$ = 34% (compared to 167% with Br_2 mixing ratio fixed).

These sensitivity simulations ~~This~~ suggested that in the MBL, Br may be a dominant GEM oxidation most of the time, but ~~occasionally~~ at times of low Br mixing ratios, O_3 could become dominant. To identify the ~~potential sources of GOM~~origin of the air masses at AI, backward trajectory analysis was conducted using the HYSPLIT4 model (https://ready.arl.noaa.gov/HYSPLIT.php). All 24 h backward trajectories started from the time of GOM daily peaks for the 50 cases. The trajectory results were clustered for over-estimation, matching, and under-estimation cases (Fig. ~~10~~5). Based on these trajectories, in about half of the 15 over-estimation cases air masses originated from marine environments, while in more than 80% of the 27 matching cases and 7 out of 8 under-estimation cases air masses came from inland northwest of AI. Note that in those under-estimation cases GOM mixing ratios were exceptionally

large, exceeding 30 ppqv.

Different source areas of air masses reaching AI could be one of the reasons for the large variation of GOM observations. The highest levels of GOM were observed in summer with RH roughly < 50% at AI (Mao et al., 2012). A close examination of the 50 cases at AI revealed low RH levels (≤ 45%) on 16 days. The time periods with RH ≤ 45% appeared mostly (78% of the time) in the afternoon over 12:00–20:00 EDT and less so (22%) at night over 21:00–02:00 EDT. During these time periods, increased GOM (15 out of 16, compared with periods with high RH on the same day) and daily maximum GOM (10 out of 16) occurred simultaneously at low RH, regardless of the time of the day.

Interestingly, the RH level of 45% corresponds to the crystallization point of NaCl (Cziczo et al., 1997; Tang et al., 1997). The crystallization of sea-salt aerosols might be link to the very high GOM peaks in certain ways. Rutter and Schauer (2007) found that particles of potassium and sodium chlorides had high partitioning coefficients that could shift the GOM gas-particle partitioning toward the aqueous phase, while ammonium sulfate, levoglucosan, and adipic acid would shift the partitioning toward the gas phase. It was thus *hypothesized* that, ~~certain processes might have been activated during transport of~~when these inland air masses reached ~~to~~ the MBL mixed with the marine air, the processes discussed above might have been activated involving the interaction between land and marine air, which potentially resulted in those very high GOM mixing ratios.

Laskin et al. (2012) found effective reactivity of chloride (Cl^-) components with organic acid in sea salt aerosols (SSAs), possibly leading to depletion of Cl^- and formation of organic salts in aerosols. Biogenic compounds in air masses originating from inland forested areas could be oxidized forming organic acids in transit. As inland air reached the MBL, these organic acids

would deposit onto SSAs and could subsequently change SSAs' chemical and physical properties, such as lowering concentrations of Cl^- and forming a thick organic film on the outside of SSAs. The lower concentrations of Cl^- and higher concentrations of organic acid in aerosols might have contributed to the shift in the gas-to-particle partitioning to the gas phase and resulted in higher GOM mixing ratios in the atmosphere.

Another possible explanation could be air masses of inland origin encountering marine air rich in atmospheric Br and BrO radicals. The main source of atmospheric Br is thought to come from the release of Br_2 and BrCl from SSA (Finlayson-Pitts, 2010; Sander et al., 2003). Experimental studies suggested Br^- enhancements of a factor of 40 to 140 on the surface of sufficiently dry artificial SSA (Ghosal et al., 2008; Hess et al., 2007). Therefore, when drier inland air masses were mixed with marine air in the MBL under relatively low RH conditions, SSA became drier, forcing more Br_2 to be released from SSA, resulting in enhanced oxidation of GEM by Br and BrO radicals. These hypotheses need to be validated in future research. These mechanisms are presently missing in the box model, leading to the model's inability to capture very high GOM mixing ratios. Measurements of halogen species and a better gas-particle partitioning mechanism are needed to better the model's performance.

3.3.2 Thompson Farm (coastal)

Generally, the box model performed well at TF (Fig. ~~8b~~2) with overall $NMSE_s$ = 0.75% and RMSE= 0.78 ppqv. Of the 12 cases at TF, ~~7~~ 6diurnal cycles of GOM (~~58~~50%) were simulated reasonably well with $NMSE_s$ < 50 %, ~~only one~~2 were~~was~~ underestimated by ~ 70 %, and 4 cases were overestimated by a factor of ~~3~~ 2to ~~6~~5. Overall, the observed average diurnal cycles of GOM for all selected summer clear-sky days at TF had daily peaks during 14:00–20:00 EDT with very low values at night between 0:00 and 8:00 EDT (Sigler et al., 2009) (Fig. ~~8b~~2). The peak observed

at 17:00 EDT (Fig. ~~8b~~2) was largely affected by the abnormally high GOM peak in that one under-estimation case (Fig. ~~9b~~4b).

For the over-estimation and matching cases, the model reproduced very low GOM mixing ratios at night (Fig. ~~9b~~4b). For the same reason substantially lowering GEM mixing ratios at night and in the early morning at TF (Mao et al., 2008), the low nighttime GOM at TF was probably caused by loss via dry deposition under nocturnal inversion. To capture these low values in model simulations, realistic nocturnal boundary layer height data were needed beside solid representation of dry deposition and chemistry in the model. The diurnal cycle of boundary layer height in the box model was parameterized based on reanalysis data obtained from the Research Data Archive at the National Center for Atmospheric Research (http://rda.ucar.edu/datasets/ds093.0/). Use of these data helped to reproduce the low nighttime GOM levels in simulations for the TF site. Another notable feature in Fig. ~~9b~~ 4b is the exceedingly high observed GOM mixing ratios in the ~~sole~~ under-estimation cases and the low observed GOM mixing ratios throughout the day in all over-estimation cases. Observed GOM mixing ratios in the under-estimation cases showed a factor of 3–~~4~~7 larger than those in the matching cases, and a factor of 3–31 larger than those in the over-estimation cases (Fig. ~~9b~~4b). Concurrently, larger fine particle concentrations, ~~8272~~ 7468 cm^{-3} on average, were observed for the under-estimation cases, which was ~~65~~ 51 and ~~93~~80% larger than those in the matching cases and over-estimation cases, respectively. Lower RH, ~~59~~66% on average, was observed in the under-estimation cases, ~~11~~ 5and ~~15~~11% lower than that in the matching and over-estimation cases, respectively. Moreover, higher air pressure (~~1017~~1018, ~~7~~ 8 and ~~10~~ 12 hPa larger than the matching and over-estimation cases, respectively), lower wind speed (~~0.59~~0.8 m s^{-1} on average, ~~47~~ 35 and ~~56~~68% lower than matching and over-estimation cases respectively), and stronger solar radiation flux (8 and 13% stronger than matching and over-estimation cases

451 respectively) were found in the under-estimation cases. An examination of the sea level pressure
452 maps (Figure S1) in ~~Clearly,~~ the under-estimation cases suggested that these cases occurred under
453 the strongest Bermuda High influence, with the calmest, sunniest, and driest conditions of all cases,
454 which is most conducive to photochemistry and pollution build-up that may have ultimately
455 contributed to the very large GOM mixing ratios in ~~that one~~those under-estimation cases. Our
456 model appeared to fail to mimic the chemistry under such conditions that produced the largest
457 GOM mixing ratios.

458 3.3.3 Pack Monadnock (inland, rural, elevated site)

459 At PM, diurnal cycles of GOM were overestimated with $NMSE_s$ = 70% and overall
460 RMSE= 0.13 ppqv. However, considering the extremely low mixing ratios of GOM observed at
461 PM (Fig. 2), cases with RMSE < 0.1 ppqv (LOD) were considered as matching cases. Therefore,
462 the model reasonably simulated 11 out of 21 (52%) cases, underestimated in ~~3~~1, and overestimated
463 in ~~7~~9. Evaluation of simulated GOM diurnal cycles against observations (Fig. ~~8c~~2) showed
464 reasonable agreement with general overestimation ranging over 0.05–0.07 ppqv.

465 The observed GOM diurnal cycle (Fig. ~~8c~~2f) showed daily maximums at 08:00 and 23:00
466 EDT, which were mainly influenced by the ~~three~~ underestimated cases (Fig. ~~9c~~4c). In comparison,
467 the remaining~~rest~~ (95~~86~~ %) ~~of the~~ cases ~~were showing~~showed a very flat ~~pattern of~~ GOM diurnal
468 cycle at PM. The first and ~~the~~ most important reason for such observation-model discrepancy is
469 that the PM site is a mountain site (700 m a.s.l.), which is above the nocturnal inversion layer
470 (~200m at TF) ~~at night~~ but within ~~the middle of~~ the convective boundary layer during the day. At
471 night, a regional pool of GOM produced ~~during daytime~~in the preceding convective boundary
472 layer remained in the residual layer, which kept the surface GOM levels from dropping below the
473 LOD at night at PM. The slight decline of GOM mixing ratios after sunrise was because of mixing

with the lower altitude air masses with depleted GOM from the night. The effect of the PM's site characteristics was not represented in the box model, which could result in model's inability to simulate diurnal variation associated with this aspect of the site. In addition, due to the dominance of GEM oxidation by O_3 in GOM production in the model, it was highly likely that the flat ~~patterns~~diurnal cycles (slightly higher at night) of GEM (Fig. 2) and O_3 were mirrored in GOM mixing ratios.

3.4 Sensitivity analysis

3.4.1 Sensitivity of GOM to physical and chemical parameters

The base ~~case~~ scenario (~~Case~~ *Scenario* 0) of these sensitivity runs represented the real atmospheric conditions on the selected 50 days at AI. ~~Case~~ *Scenarios* 1–10 are sensitivity ~~cases~~ runs where one parameter in the base ~~case~~ scenario was changed at the time (Table 3). ~~Case~~ *Scenario* 1 turned off photolysis reactions. ~~Cases~~ *Scenarios* 2–4 tested the gas-particle partitioning scheme. The liquid water content range was derived from Hedgecock et al. (2003). ~~Cases~~ *Scenarios* 5–~~8~~ 9tested the sensitivity of GOM mixing ratios to GEM oxidation reactions and their coefficients. ~~Cases~~ *Scenarios* ~~9~~10–~~10~~–11 tested the sensitivity of GOM mixing ratios to temperature. The temperature range was based on the observed average temperature diurnal cycle.

The importance of photochemical radicals in GEM oxidation was demonstrated clearly in decreases of ~~21–80~~3-92 and ~~28–92~~2-100 % in daytime GOM and PBM, respectively with largest decreases at noon as a result of turning off photochemistry (~~*Case*~~ *Scenario 1*). *Scenario*~~*Case*~~ *2* showed ~74% of oxidized Hg transformed to PBM at AI with gas-particle partitioning switched on. In this ~~case~~scenario, HgO and $Hg(OH)_2$ were more sensitive than halogenated GOM species (such as ~~BrHgOOH and BrHgOBr~~ $BrHgNO_2$). Turning off gas-particle partitioning more than

quadrupled the mixing ratios of HgO and $Hg(OH)_2$ throughout the day compared to increases of more than 100 and 60% halogenated GOM species during daytime and nighttime, respectively.

Decreasing liquid water content by 1 order of magnitude tripled GOM mixing ratios, whereas increasing the same amount decreased GOM by ~~87~~80% (~~*Cases* *Scenarios* *3–4*~~). Sensitivity of GOM and PBM mixing ratios to dominant GEM oxidation reactions are shown in ~~*Cases* *Scenarios* *5–8*~~. Using the slowest rate coefficient of GEM + O_3 obtained from Hall (1995), as opposed to the one from Snider et al. (2008) led to a decrease of 56.7% in HgO, and decreases of 15 and 85% in total GOM during daytime and nighttime, respectively. Using an order of magnitude faster rate coefficient of GEM + Br from Ariya et al. (2002) increased 250% of total GOM during daytime. Turning off GEM oxidation by O_3, OH, or Br resulted in decreases of ~~19~~16, 10, and ~~30~~48%, respectively, in daytime GOM mixing ratios. Turning off the GEM + Br oxidation reaction also decreased daytime PBM mixing ratios by ~~45~~60%. However, for nighttime GOM and PBM mixing ratios, turning off the GEM + O_3 reaction caused decreases of ~~92~~ 88 and 51%, respectively, since Br and OH are both photochemical radicals and O_3 was the predominant oxidant for GEM in the model.

~~*Cases* *Scenarios* *9–10*~~ 11 suggested that nighttime GOM and PBM mixing ratios were more sensitive to temperature than those during daytime. Increasing temperature by 10 K caused a 9% increase each in GOM and PBM mixing ratios during daytime but a decrease of 13% in GOM and 54% in PBM at night. This was because the rate coefficient of GEM + O_3 increases with increasing temperature, but the rate coefficient of GEM + OH decreases with increasing temperature.

In summary, the parameters used in gas-particle partitioning process, including solar radiation values, temperature, and the rate coefficients of major GEM oxidation reaction, could all

affect the GOM simulation but with varying degree. Aerosol properties were suggested to play a very important role in the partitioning of ambient GOM and PBM species and thus should be better represented in future Hg model simulation studies. Using a slower rate coefficient of GEM + O_3 (Hall, 1995) had similar effects as not including the GEM + O_3 reaction, i.e. decreasing GOM mixing ratios, especially at nighttime, and brominated GOM species becoming dominant. The GEM + OH reaction was not as important as GEM + O_3 or Br. The use of a higher GEM + Br rate coefficient derived from the study by Ariya et al. (2002) caused more than a factor of 3 higher GOM and PBM resulting in overestimated GOM for most cases. GOM and PBM production appeared to favor lower temperature at daytime and higher temperature at night, and simulated GOM concentrations were not as sensitive to temperature change as to solar radiation and gas-particle partitioning.

3.4.2 Influence of physical and chemical processes on GOM diurnal cycle

Large variations were exhibited in both observed ~~(Fig. 2)~~ and simulated ~~(Fig. 3)~~ GOM mixing ratios at AI, TF, and PM (Fig. 2). Considering that all cases were under relatively calm, clear-sky conditions, the simulated GOM mixing ratio and diurnal cycle were controlled primarily by chemical reactions, dry deposition, and gas-particle partitioning. To quantify the contribution of processes to the difference of GOM mixing ratios at the three sites, ~~three~~ two sensitivity ~~cases~~ scenarios were conducted: ~~at TF and PM: (1) use the same dry deposition velocity and boundary layer height as those of AI for TF (denoted as TF_AIdry) and PM (denoted as PM_AIdry); (2) use the same gas-particle partitioning parameters as those of AI for TF (denoted as TF_AIaero) and PM (denoted as PM_AIaero); (3)~~ use the same physical parameters as those of AI for TF (denoted as TF_AIaerodry) and PM (denoted as PM_AIaerodry).

Comparison of simulated GOM diurnal cycles from the AI, TF_AIaerodry and PM_AIaerodry scenario~~case~~s showed the influence of different chemical scenarios on GOM mixing ratios at the three sites. At night, GOM mixing ratios at the three sites did not vary significantly (0-2 ppqv), with higher values at PM than those at AI and TF (Fig. ~~5~~6). However, the mid-day peak at AI was more than a factor of two greater ~~more than one order of magnitude higher~~ than those in the PM_AIaerodry and TF_AIaerodry ~~cases~~scenarios, indicating more chemical transformation of Hg occurring at AI. The daytime mixing ratios of GOM at TF and PM were similar, while the nighttime GOM mixing ratios at PM were 30-52% higher than at AI and 20-200% higher than at TF. This probably resulted from larger nighttime GEM and O_3 mixing ratios, hence producing more GOM, at PM than ~~those~~ at TF and AI. Specifically, nighttime GEM mixing ratios at PM were 8-15% higher than at AI and 8-34% higher than TF cases, while nighttime O_3 mixing ratios at PM were 11-70% larger than at AI and 35-260% larger than at TF. PM had higher nighttime GEM and O_3 mixing ratios, because this site was exposed in the residual boundary layer at night due to its high elevation, constantly replenished with the regional pool of air from the preceding convective boundary layer~~daytime~~. Overall, chemical transformation contributed ~60% of the daytime difference in GOM between AI and the two sites over land (TF and PM), 33% of the nighttime difference between AI and TF, and 26% of the difference between PM and AI.

In summary, the sensitivity scenarios suggested that ~~D~~dry deposition and gas-particle partitioning contributed 4-37% and 30-96%, respectively, of the total GOM difference between AI and PM. Both processes had larger contributions at night that during daytime. Dry deposition contributed 6-24% of the GOM difference between AI and TF and gas-particle partitioning 18-78%.

3.4.3 Br chemistry in the MBL

Diurnal cycles of Br and BrO radicals (Fig. 7~~6~~) were simulated using the Br chemical mechanism described in Sect. 2. Photodissociation of Br_2 was the main source of Br and BrO radicals during daytime. Our simulations suggested that reactive Br compounds were significant gaseous oxidants of GEM in the MBL at a fixed initial mixing ratio of 5.6 ppqv for Br_2. Increasing initial mixing ratios of Br_2 by 25% resulted in an increase of 0.01–2.15 ppqv in GOM mixing ratios.

In addition, the reaction of BrO with methyldioxy (CH_3O_2) radicals could have important influence on the mixing ratios of Br, BrO, and GOM. Simulated daytime mixing ratios of CH_3O_2 was ~ 40 pptv, and the rate coefficient of $(5.7\pm0.6) \times 10^{-12}$ cm^3 $molecule^{-1}$ s^{-1} at 298 K for BrO + CH_3O_2 (Aranda et al., 1997~~a~~) was used for our simulations. Pathways B1, B2, and B3 were suggested by Aranda et al. (1997~~a~~) based on an experimental study (Table 4). However, the production of CH_3O may be due to its self-reaction in B1. Guha and Francisco (2003) suggested CH_3OOOBr to be a likely intermediate of this reaction, and that CH_3OOOBr could dissociate to CH_2O+HOOBr (B4, Table 4). Based on thermodynamics calculations, CH_3OBr and O_2 (B3, Table 4) were possible products. BrOO and HOBr were both included in the Br chemical cycle and can be transformed back to Br and BrO radicals in the model. However, it is unclear whether CH_3OBr (product of B3) or HOOBr (product of B4) could be transformed back to Br and BrO radicals in the atmosphere. In this case, using the B3 or B4 pathway did not appear to make a difference in our box model results.

In this study, the B1 and B2 pathways were used for the CH_3O_2 +BrO reaction as part of the base ~~case simulation~~ scenario (denoted as Sim-avg BrOO). The sensitivity ~~case~~ run Sim-avg CH_3OBr used the B3 pathway in lieu of B1 and B2. The simulated average and the range of GOM diurnal cycles in the base ~~case~~ and ~~the~~ sensitivity ~~case~~ scenarios were evaluated against observed mean and median GOM diurnal cycles of the 50 study cases at AI (Fig. 7~~8~~). If the CH_3O_2 +BrO

reaction followed the B1 and B2 pathways, this reaction had a negligible effect on reactive Br radicals. However, if B3 or B4 was applied, the simulated total GOM mixing ratio was lowered by 50% during daytime. Moreover, the simulated GOM diurnal cycle in the base ~~case~~ scenario agreed favorably with the observed average GOM diurnal cycle (NMSE= 15 %), while the results of the Sim-avg CH_3OBr ~~case~~ scenario were in better agreement with the observed median GOM diurnal cycle (NMSE= 14%). These agreements indicated that, if the $BrO+CH_3O_2$ reaction was a net sink of BrO radicals, the model was able to simulate ~~better~~ most cases better, whereas if the product of $BrO+CH_3O_2$ was transformed back to Br or BrO radicals, the model appeared to capture those cases with large GOM mixing ratios (> 6 ppqv). Due to the scarcity of kinetic research on the B3 and B4 pathways, we used B1 and B2 pathways for CH_3O_2 +BrO reaction in this study.

In ~~summary~~short, the pathways of $BrO+CH_3O_2$ could play an important role in atmospheric Br chemistry and Hg speciation in Br-rich environments. Research on the reaction pathways and rate coefficients of the $BrO+CH_3O_2$ reaction is warranted to better assess the role of this reaction.

4 Summary

This study provided a state-of-the-art chemical mechanism with most up-to-date Hg and halogen chemistry ~~for atmospheric Hg modeling system~~ and tested the ~~chemical~~ mechanism for three different environments using a mercury box model. Eighty-three summer clear-sky days were selected at marine, coastal, and inland elevated sites in southern New Hampshire to evaluate the model. As a result, for each of the three environments, GOM diurnal cycles of over half selected cases were reasonably represented by the box model. It was hypothesized, based on the key results and discussion presented in Section 3, that dry air masses with organic compounds transported from inland may result in very large GOM mixing ratios in the MBL possibly due to changing physical and chemical properties of sea salt aerosols. The low nighttime and morning GOM mixing

ratios at coastal site were likely a result of a net loss due to dry deposition in the nocturnal inversion layer. The GOM mixing ratios above the ~~limit of detection~~LOD at the inland site at night were probably caused by constant replenishment from a regional pool, in the residual boundary layer, of GOM that was produced in the preceding daytime convective boundary layer. The updated chemical mechanism largely improved the simulation of the magnitude and pattern of GOM diurnal ~~cycle~~ variation ~~simulations~~ at the coastal and inland sites. HgO produced from oxidation of GEM by O_3 and OH dominated GOM species at the coastal and inland sites, while bromine-induced mercury species (mainly BrHgOOH, BrHgOBr, and HgBrO) were important at the marine site. In Br chemistry, the products of the CH_3O_2 +BrO reaction strongly influenced the simulated Br and Hg concentrations. In this study, GEM oxidation by O_3 and OH was represented in ways similar to those in regional and global models, which is limited by the current nebulous understanding of potential surface chemistry.

It should be noted that without measurements of speciated GOM, modeling results cannot be used to conclusively identify the dominant oxidants of Hg, as well as dominant GOM species in that matter, in the atmosphere. Indeed, the potential uncertainty in ambient Hg measurements especially GOM is a major concern in the community. That being said, it is unlikely to have a quantitative understanding of the bias of our GOM concentrations. Recent laboratory experiments and reviews (Lyman et al., 2010; Jaffe et al., 2014; McClure et al., 2014; Huang and Gustin, 2015; Gustin et al., 2015) reported O_3 and relative humidity (RH) interferences on mercury halides for KCl-coated denuder, the part of Tekran 1130 unit commonly used for GOM field measurements. As stated in Section 2, in our GOM measurement the RH effect was minimized by adding refrigeration to remove excess of water in the airsteam. O_3 interference and bias low GOM collection efficiency of KCl-coated denuders were limited to a handful of GOM species in

laboratory experiments and remain untested in field measurements. If the measured GOM concentrations were indeed biased low by a factor of 2 or 3 under certain conditions as previous studies speculated, the matching cases at AI and TF would be reduced from 50% of the total cases to 30%, and the model would potentially underestimate GOM concentrations in the remaining cases (70%) by a factor of 3 to 4. It is however hard to speculate the effect at PM since most GOM observations there were below the LOD. This suggested even greater unknowns in our understanding of Hg chemistry. Therefore, ~~It should also be acknowledged that studies have suggested problems in GOM measurements using the current Tekran instruments (Gustin et al., 2015; Jaffe et al., 2014). If indeed real atmospheric GOM concentrations were underestimated in Tekran measurements, it implies even more confounding, yet unknown issues in our current understanding of Hg chemistry. M~~more experimental or theoretical studies on Hg reactions and better GOM measurement data are warranted to improve our understanding and subsequently model simulations of atmospheric Hg cycling, which can ultimately serve policy-making in an effective manner.

Acknowledgements

This work is funded by NSF AGS grant # 1141713. We thank T. Dibble, Y. Zhou, Y. Zhang, and C. B. Hall for valuable suggestions and help. We are grateful to the three anonymous reviewers for their thoughtful, detailed, constructive comments, which helped to improve the clarity of the paper.

References

Aranda, A., Le Bras, G., La Verdet, G., and Poulet, G.: The BrO + CH_3O_2 reaction: kinetics and role in the atmospheric ozone budget, Geophys. Res. Lett., 24, 2745–2748, 1997.

Ariya, P. A., Khalizov, A., and Gidas, A.: Reactions of gaseous mercury with atomic and molecular halogens: kinetics, product studies, and atmospheric implications, J. Phys. Chem. A, 106, 7310–7320, 2002.

Ariya, P. A., Amyot, M., Dastoor, A., Deeds, D., Feinberg, A., Kos, G., Poulain, A., Ryjkov, A., Semeniuk, K., Subir, M., and Toyota, K.: Mercury physicochemical and biogeochemical transformation in the atmosphere and at atmospheric interfaces: a review and future directions, Chem. Rev., 115, 3760–3802, doi:10.1021/cr500667e, 2015.

Atkinson, R., Baulch, D. L., Cox, R. A., Crowley, J. N., Hampson, R. F., Hynes, R. G., Jenkin, M. E., Rossi, M. J., and Troe, J.: Evaluated kinetic and photochemical data for atmospheric chemistry: Volume I – gas phase reactions of Ox, HOx, NOx and SOx species, Atmos. Chem. Phys., 4, 1461–1738, doi:10.5194/acp-4-1461-2004, 2004.

Atkinson, R., Baulch, D. L., Cox, R. A., Crowley, J. N., Hampson, R. F., Hynes, R. G., Jenkin, M. E., Rossi, M. J., Troe, J., and Wallington, T. J.: Evaluated kinetic and photochemical data for atmospheric chemistry: Volume IV – gas phase reactions of organic halogen species, Atmos. Chem. Phys., 8, 4141–4496, doi:10.5194/acp-8-4141-2008, 2008.

Balabanov, N. B., Shepler, B. C., and Peterson, K. A.: Accurate global potential energy surface and reaction dynamics for the ground state of $HgBr_2$, J. Phys. Chem. A, 109, 8765–8773, 2005.

Baumgardner, D., Raga, G. B., Kok, G., Ogren, J., Rosas, I., Báez, A., and Novakov, T.: On the evolution of aerosol properties at a mountain site above Mexico City, J. Geophys. Res. -Atmos., 105, 22243–22253, doi: 10.1029/2000JD900299, 2000.

Bergan, T. and Rodhe, H.: Oxidation of elemental mercury in the atmosphere; constraints imposed by global scale modelling, J. Atmos. Chem., 40, 191–212, 2001.

Bergan, T., Gallardo, L., and Rodhe, H.: Mercury in the global troposphere: a three-dimensional model study, Atmos. Environ., 33, 1575–1585, 1999.

Chang, J. C. and Hanna, S. R.: Air quality model performance evaluation, Meteorol. Atmos. Phys., 87, 167–196, doi: 10.1007/s00703-003-0070-7, 2004.

Clarkson, T. W.: The toxicity of mercury and its compounds, in: Mercury Pollution: Integration and Synthesis, edited by: Watras, C. J. and Huckabee, J.W., Boca Raton, FL, USA, 631–641, 1994.

Cziczo, D. J., Nowak, J. B., Hu, J. H., and Abbatt, J. P. D.: Infrared spectroscopy of model tropospheric aerosols as a function of relative humidity: observation of deliquescence and crystallization, J. Geophys. Res.-Atmos., 102, 18843–18850, 1997.

688 Dibble, T. S., Zelie, M. J., and Mao, H.: Thermodynamics of reactions of ClHg and BrHg radicals
689 with atmospherically abundant free radicals, Atmos. Chem. Phys., 12, 10271–10279,
690 doi:10.5194/acp-12-10271-2012, 2012.

691 Donohoue, D. L., Bauer, D., and Hynes, A. J.: Temperature and pressure dependent rate
692 coefficients for the reaction of Hg with Cl and the reaction of Cl with Cl: a pulsed laser
693 photolysispulsed laser induced fluorescence Study, J. Phys. Chem. A, 109, 7732–7741, 2005.

694 Finlayson-Pitts, B. J.: Halogens in the troposphere, Anal. Chem., 82, 770–776, doi:
695 10.1021/ac901478p, 2010.

696 Finley, B. D. and Saltzman, E. S.: Observations of Cl_2, Br_2, and I_2 in coastal marine air, J. Geophys.
697 Res., 113(D21), D21301, doi:10.1029/2008JD010269, 2008.

698 Fischer, E. V., Ziemba, L. D., Talbot, R.W., Dibb, J. E., Griffin, R. J., Husain, L., and Grant, A.
699 N.: Aerosol major ion record at Mount Washington, J. Geophys. Res.-Atmos., 112, D02303, doi:
700 10.1029/2006JD007253, 2007.

701 Ghosal, S., Brown, M. A., Bluhm, H., Krisch, M. J., Salmeron, M., Jungwirth, P., and Hemminger,
702 J. C.: Ion partitioning at the liquid/vapor interface of a multicomponent alkali halide solution: a
703 model for aqueous sea salt aerosols, J. Phys. Chem. A, 112, 12378–12384, 2008.

704 Glasow, R. V., Sander, R., Bott, A., and Crutzen, P. J.: Modeling halogen chemistry in the marine
705 boundary layer 1. Cloud-free MBL, J. Geophys. Res.-Atmos., 107, 9-1–9-16, 2002.

706 Goodsite, M. E., Plane, J. M. C., and Skov, H.: A theoretical study of the oxidation of HgO to
707 $HgBr_2$ in the troposphere, Environ. Sci. Technol., 38, 1772–1776, 2004.

708 Goodsite, M. E., Plane, J. M. C., and Skov, H.: Erratum: A theoretical study of the oxidation of
709 HgO to $HgBr_2$ in the troposphere, (Environ. Sci. Technol. (2004) 38:6 (1772–1776) doi:
710 10.1021/es034680s), Environ. Sci. Technol., 46, 5262, doi: 10.1021/es301201c, 2012.

711 Guha, S. and Francisco, J. S.: An ab initio study of the pathways for the reaction between CH_3O_2
712 and BrO radicals, J. Chem. Phys., 118, 1779–1793, doi:10.1063/1.1531099, 2003.

713 Gustin, M. S., Huang, J., Miller, M. B., Peterson, C., Jaffe, D. A., Ambrose, J., Finley, B. D.,
714 Lyman, S. N., Call, K., Talbot, R., Feddersen, D., Mao, H. and Lindberg, S. E.: Do we understand
715 what the mercury speciation instruments are actually measuring? Results of RAMIX,
716 Environmental Science and Technology, 47(13), 7295–7306, 2013.

717 Gustin, M. S., Amos, H. M., Huang, J., Miller, M. B., and Heidecorn, K.: Measuring and modeling
718 mercury in the atmosphere: a critical review, Atmos. Chem. Phys., 15, 5697–5713, doi:
719 10.5194/acp-15-5697-2015, 2015.

720 Hall, B.: The gas phase oxidation of elemental mercury by ozone, Water Air Soil Poll., 80, 301–
721 315, 1995.

Hanna, S. R.: Air quality model evaluation and uncertainty, JAPCA J. Air Waste Ma., 38, 406–412, doi: 10.1080/08940630.1988.10466390, 1988.

Hanna, S. R., Strimaitis, D. G., and Chang, J. C.: Hazard response modeling uncertainty (a quantitative method), vol. I: User's guide for software for evaluating hazardous gas dispersion models; vol. II: Evaluation of commonly-used hazardous gas dispersion models; vol. III: Components of uncertainty in hazardous gas dispersion models, Sigma Research Corporation, Westford, USA, 1991.

Hanna, S. R., Chang, J. C., and Strimaitis, D. G.: Hazardous gas model evaluation with field observations, Atmos. Environ. A-Gen., 27, 2265–2285, doi: 10.1016/0960-1686(93)90397-H, 1993.

Hedgecock, I. M. and Pirrone, N.: Chasing quicksilver: modeling the atmospheric lifetime of Hg^0 (g) in the marine boundary layer at various latitudes, Environ. Sci. Technol., 38, 69–76, 2004.

Hedgecock, I. M. and Pirrone, N.: Modelling chemical and physical processes of Hg compounds in the marine boundary layer, Dyn. Mercury Pollut. Reg. Glob. Scales Atmospheric Process. Hum. Expo. World, 2005.

Hedgecock, I. M., Pirrone, N., Sprovieri, F., and Pesenti, E.: Reactive gaseous mercury in the marine boundary layer: modelling and experimental evidence of its formation in the Mediterranean region, Atmos. Environ., 37, S41–S49, 2003.

Hess, M., Krieger, U. K., Marcolli, C., Huthwelker, T., Ammann, M., Lanford, W. A., and Peter, T.: Bromine enrichment in the near-surface region of Br-doped NaCl single crystals diagnosed by rutherford backscattering spectrometry, J. Phys. Chem. A, 111, 4312–4321, 2007.

Holmes, C. D., Jacob, D. J., and Yang, X.: Global lifetime of elemental mercury against oxidation by atomic bromine in the free troposphere, Geophys. Res. Lett., 33, L20808, doi: 10.1029/2006GL027176, 2006.

Holmes, C. D., Jacob, D. J., Mason, R. P., and Jaffe, D. A.: Sources and deposition of reactive gaseous mercury in the marine atmosphere, Atmos. Environ., 43, 2278–2285, 2009.

Holmes, C. D., Jacob, D. J., Corbitt, E. S., Mao, J., Yang, X., Talbot, R., and Slemr, F.: Global atmospheric model for mercury including oxidation by bromine atoms, Atmos. Chem. Phys., 10, 12037–12057, doi:10.5194/acp-10-12037-2010, 2010.

Huang, J., Miller, M. B., Weiss-Penzias, P. and Gustin, M. S.: Comparison of gaseous oxidized Hg measured by KCl-coated denuders, and nylon and cation exchange membranes, Environmental Science and Technology, 47(13), 7307–7316, 2013.

Jaffe, D. A., Lyman, S., Amos, H. M., Gustin, M. S., Huang, J., Selin, N. E., Levin, L., ter Schure, A., Mason, R. P., Talbot, R., Rutter, A., Finley, B., Jaeglé, L., Shah, V., McClure, C., Ambrose, J., Gratz, L., Lindberg, S., Weiss-Penzias, P., Sheu, G.-R., Feddersen, D., Horvat, M., Dastoor, A., Hynes, A. J., Mao, H., Sonke, J. E., Slemr, F., Fisher, J. A., Ebinghaus, R., Zhang, Y., and Edwards,

G.: Progress on understanding atmospheric mercury hampered by uncertain measurements, Environ. Sci. Technol., 48, 7204–7206, doi: 10.1021/es5026432, 2014.

Kim, P.-R., Han, Y.-J., Holsen, T. M., and Yi, S.-M.: Atmospheric particulate mercury: concentrations and size distributions, Atmos. Environ., 61, 94–102, 2012.

Kim, S. Y., Talbot, R., Mao, H., Blake, D. R., Huey, G., and Weinheimer, A. J.: Chemical transformations of Hg during Arctic mercury depletion events sampled from the NASA DC-8, Atmos. Chem. Phys. Discuss., 10, 10077–10112, doi: 10.5194/acpd-10-10077-2010, 2010.

Kutsher, J., Haikin, N., Sharon, A., and Heifetz, E.: On the formation of an elevated nocturnal inversion layer in the presence of a low-level jet: a case study, Bound.-Lay. Meteorol., 144, 441–449, doi:10.1007/s10546-012-9720-y, 2012.

Laskin, A., Moffet, R. C., Gilles, M. K., Fast, J. D., Zaveri, R. A., Wang, B., Nigge, P., and Shutthanandan, J.: Tropospheric chemistry of internally mixed sea salt and organic particles: surprising reactivity of NaCl with weak organic acids, J. Geophys. Res.-Atmos., 117, D15302, doi: 10.1029/2012JD017743, 2012.

Laurier, F. and Mason, R.: Mercury concentration and speciation in the coastal and open ocean boundary layer, J. Geophys. Res.-Atmos., 112, D06302, doi: 10.1029/2006JD007320, 2007.

Laurier, F. J. G., Mason, R. P., Whalin, L., and Kato, S.: Reactive gaseous mercury formation in the North Pacific Ocean's marine boundary layer: a potential role of halogen chemistry, J. Geophys. Res.-Atmos., 108, ACH3-1—ACH3-12, doi: 10.1029/2003JD003625, 2003.

Lewis, E. R. and Schwartz, S. E.: Comment on "Size distribution of sea-salt emissions as a function of relative humidity," Atmos. Environ., 40, 588–590, doi: 10.1016/j.atmosenv.2005.08.043, 2006.

Lin, C.-J. and Pehkonen, S. O.: Aqueous phase reactions of mercury with free radicals and chlorine: implications for atmospheric mercury chemistry, Chemosphere, 38, 1253–1263, 1999.

Lin, C.-J., Pongprueksa, P., Lindberg, S. E., Pehkonen, S. O., Byun, D., and Jang, C.: Scientific uncertainties in atmospheric mercury models I: Model science evaluation, Atmos. Environ., 40, 2911–2928, 2006.

Lindberg, S. E., Brooks, S., Lin, C.-J., Scott, K. J., Landis, M. S., Stevens, R. K., Goodsite, M., and Richter, A.: Dynamic oxidation of gaseous mercury in the arctic troposphere at polar sunrise, Environ. Sci. Technol., 36, 1245–1256, 2002.

Madronich, S.: UV radiation in the natural and perturbed atmosphere, in: Environmental Effects of UV, CRC Press, Boca Raton, FL, USA, available at: http://opensky.library.ucar.edu/collections/OSGC-000-000-020-698 (last access: 16 April 2015), 1993.

Mao, H. and Talbot, R.: O_3 and CO in New England: temporal variations and relationships, J. Geophys. Res.-Atmos., 109, D21304, doi: 10.1029/2004JD004913, 2004.

Mao, H., Talbot, R. W., Sigler, J. M., Sive, B. C., and Hegarty, J. D.: Seasonal and diurnal variations of Hg over New England, Atmos. Chem. Phys., 8, 1403–1421, doi: 10.5194/acp-8-1403-2008, 2008.

Mao, H., Talbot, R., Hegarty, J., and Koermer, J.: Speciated mercury at marine, coastal, and inland sites in New England – Part 2: Relationships with atmospheric physical parameters, Atmos. Chem. Phys., 12, 4181–4206, doi: 10.5194/acp-12-4181-2012, 2012.

Mason, R. P., Kim, E.-H., Cornwell, J., and Heyes, D.: An examination of the factors influencing the flux of mercury, methylmercury and other constituents from estuarine sediment, Mar. Chem., 102, 96–110, 2006.

Miller, C. L., Mason, R. P., Gilmour, C. C., and Heyes, A.: Influence of dissolved organic matter on the complexation of mercury under sulfidic conditions, Environ. Toxicol. Chem., 26, 624–633, 2007.

Moldanová, J. and Ljungström, E.: Sea-salt aerosol chemistry in coastal areas: a model study, J. Geophys. Res.-Atmos., 106, 1271–1296, doi: 10.1029/2000JD900462, 2001.

Obrist, D., Tas, E., Peleg, M., Matveev, V., Faïn, X., Asaf, D., and Luria, M.: Bromine-induced oxidation of mercury in the mid-latitude atmosphere, Nat. Geosci., 4, 22–26, 2011.

Pal, B. and Ariya, P. A.: Gas-phase HO-initiated reactions of elemental mercury: kinetics, product studies, and atmospheric implications, Environ. Sci. Technol., 38, 5555–5566, 2004a.

Pal, B. and Ariya, P. A.: Studies of ozone initiated reactions of gaseous mercury: kinetics, product studies, and atmospheric implications, Phys. Chem. Chem. Phys., 6, 572–579, 2004b.

Pillai, P. S. and Moorthy, K. K.: Aerosol mass-size distributions at a tropical coastal environment: response to mesoscale and synoptic processes, Atmos. Environ., 35, 4099–4112, doi: 10.1016/S1352-2310(01)00211-4, 2001.

Poissant, L., Pilote, M., Beauvais, C., Constant, P. and Zhang, H. H.: A year of continuous measurements of three atmospheric mercury species (GEM, RGM and Hgp) in southern Québec, Canada, Atmospheric Environment, 39(7), 1275–1287, 2005.

Raofie, F. and Ariya, P. A.: Product study of the gas-phase BrO-initiated oxidation of Hg^0: Evidence for stable Hg^{1+} compounds, Environ. Sci. Technol., 38, 4319–4326, 2004.

Rolfhus, K. R., Sakamoto, H. E., Cleckner, L. B., Stoor, R. W., Babiarz, C. L., Back, R. C., Manolopoulos, H., and Hurley, J. P.: Distribution and fluxes of total and methylmercury in Lake Superior, Environ. Sci. Technol., 37, 865–872, 2003.

Rutter, A. P. and Schauer, J. J.: The impact of aerosol composition on the particle to gas partitioning of reactive mercury, Environ. Sci. Technol., 41, 3934–3939, doi: 10.1021/es062439i, 2007.

827 Rutter, A. P., Shakya, K. M., Lehr, R., Schauer, J. J., and Griffin, R. J.: Oxidation of gaseous
828 elemental mercury in the presence of secondary organic aerosols, Atmos. Environ., 59, 86–92,
829 2012.

830 Saiz-Lopez, A. and von Glasow, R.: Reactive halogen chemistry in the troposphere, Chem. Soc.
831 Rev., 41, 6448–6472, doi: 10.1039/C2CS35208G, 2012.

832 Saiz-Lopez, A., Shillito, J. A., Coe, H., and Plane, J. M. C.: Measurements and modelling of I_2,
833 IO, OIO, BrO and NO_3 in the mid-latitude marine boundary layer, Atmos. Chem. Phys., 6, 1513–
834 1528, doi:10.5194/acp-6-1513-2006, 2006.

835 Sander, R., Keene, W. C., Pszenny, A. A. P., Arimoto, R., Ayers, G. P., Baboukas, E., Cainey, J.
836 M., Crutzen, P. J., Duce, R. A., Hönninger, G., Huebert, B. J., Maenhaut, W., Mihalopoulos, N.,
837 Turekian, V. C., and Van Dingenen, R.: Inorganic bromine in the marine boundary layer: a critical
838 review, Atmos. Chem. Phys., 3, 1301–1336, doi:10.5194/acp-3-1301-2003, 2003.

839 Sander, S. P., Abbatt, J., Barker, J. R., Burkholder, J. B., Friedl, R. R., Golden, D. M., Huie, R. E.,
840 Kolb, C. E., Kurylo, M. J., Moortgat, G. K., Orkin, V. L., and Wine, P. H.: Chemical Kinetics and
841 Photochemical Data for Use in Atmospheric Studies, Evaluation No. 17, JPL Publication 10-6, Jet
842 Propulsion Laboratory, Pasadena, available at: http://jpldataeval.jpl.nasa.gov, 2011.

843 Sandu, A. and Sander, R.: Technical note: Simulating chemical systems in Fortran90 and Matlab
844 with the Kinetic PreProcessor KPP-2.1, Atmos. Chem. Phys., 6, 187–195, doi: 10.5194/acp-6-187-
845 2006, 2006.

846 Schroeder, W. H. and Munthe, J.: Atmospheric mercury – an overview, Atmos. Environ., 32, 809–
847 822, 1998.

848 Schwartz, S. E.: Mass-transport considerations pertinent to aqueous phase reactions of gases in
849 liquid-water clouds, in: Chemistry of Multiphase Atmospheric Systems, edited by: Jaeschke, D.
850 W., Springer, Berlin, Heidelberg, 415–471, available at: http://link.springer.com/
851 chapter/10.1007/978-3-642-70627-1_16 (last access: 17 April 2015), 1986.

852 Selin, N. E., Javob, D. J., Park, R. J., Yantosca, R. M., Strode, S., Jaeglé, L., and Jaffe, D.:
853 Chemical cycling and deposition of atmospheric mercury: global constraints from observations, J.
854 Geophys. Res.-Atmos., 112, D02308, doi: 10.1029/2006JD007450, 2007.

855 Seigneur, C., Wrobel, J. and Constantinou, E.: A chemical kinetic mechanism for atmospheric
856 inorganic mercury, Environmental Science and Technology, 28(9), 1589–1597, 1994.

857 Shon, Z.-H., Kim, K.-H., Kim, M.-Y., and Lee, M.: Modeling study of reactive gaseous mercury
858 in the urban air, Atmos. Environ., 39, 749–761, 2005.

859 Sigler, J. M., Mao, H., and Talbot, R.: Gaseous elemental and reactive mercury in Southern New
860 Hampshire, Atmos. Chem. Phys., 9, 1929–1942, doi:10.5194/acp-9-1929-2009, 2009.

Sillman, S., Marsik, F. J., Al-Wali, K. I., Keeler, G. J., and Landis, M. S.: Reactive mercury in the troposphere: model formation and results for Florida, the northeastern United States, and the Atlantic Ocean, J. Geophys. Res.-Atmos., 112, D23305, doi: 10.1029/2006JD008227, 2007.

Simpson, W. R., von Glasow, R., Riedel, K., Anderson, P., Ariya, P., Bottenheim, J., Burrows, J., Carpenter, L. J., Frieß, U., Goodsite, M. E., Heard, D., Hutterli, M., Jacobi, H.-W., Kaleschke, L., Neff, B., Plane, J., Platt, U., Richter, A., Roscoe, H., Sander, R., Shepson, P., Sodeau, J., Steffen, A., Wagner, T., and Wolff, E.: Halogens and their role in polar boundary layer ozone depletion, Atmos. Chem. Phys., 7, 4375–4418, doi:10.5194/acp-7-4375-2007, 2007.

Simpson, W. R., Brown, S. S., Saiz-Lopez, A., Thornton, J. A., and von Glasow, R.: Tropospheric halogen chemistry: sources, cycling, and impacts, Chem. Rev., 115, 4035–4062, doi: 10.1021/cr5006638, 2015.

Snider, G., Raofie, F., and Ariya, P. A.: Effects of relative humidity and CO (g) on the O_3-initiated oxidation reaction of HgO (g): kinetic and product studies, Phys. Chem. Chem. Phys., 10, 5616–5623, 2008.

Soerensen, A. L., Sunderland, E. M., Holmes, C. D., Jacob, D. J., Yantosca, R. M., Skov, H., Christensen, J. H., Strode, S. A., and Mason, R. P.: An improved global model for air–sea exchange of mercury: high concentrations over the North Atlantic, Environ. Sci. Technol., 44, 8574–8580, 2010.

Steffen, A., Douglas, T., Amyot, M., Ariya, P., Aspmo, K., Berg, T., Bottenheim, J., Brooks, S., Cobbett, F., Dastoor, A., Dommergue, A., Ebinghaus, R., Ferrari, C., Gardfeldt, K., Goodsite, M. E., Lean, D., Poulain, A. J., Scherz, C., Skov, H., Sommar, J., and Temme, C.: A synthesis of atmospheric mercury depletion event chemistry in the atmosphere and snow, Atmos. Chem. Phys., 8, 1445–1482, doi:10.5194/acp-8-1445-2008, 2008.

Subir, M., Ariya, P. A., and Dastoor, A. P.: A review of uncertainties in atmospheric modeling of mercury chemistry I. Uncertainties in existing kinetic parameters – fundamental limitations and the importance of heterogeneous chemistry, Atmos. Environ., 45, 5664–5676, 2011.

Talbot, R., Mao, H., and Sive, B.: Diumal characteristics of surface level O_3 and other important trace gases in New England, J. Geophys. Res., 1 10, D09307, doi: 10.1029/2004JD005449, 2005.

Tang, I. N., Tridico, A. C., and Fung, K. H.: Thermodynamic and optical properties of sea salt aerosols, J. Geophys. Res.-Atmos., 102, 23269–23275, 1997.

Tokos, J. J. S., Hall, B., Calhoun, J. A., and Prestbo, E. M.: Homogeneous gas-phase reaction of HgO with H_2O_2, O_3, CH_3I, and $(CH_3)_2S$: implications for atmospheric Hg cycling, Atmos. Environ., 32, 823–827, 1998.

Toyota, K., McConnell, J. C., Staebler, R. M., and Dastoor, A. P.: Air–snowpack exchange of bromine, ozone and mercury in the springtime Arctic simulated by the 1-D model PHANTAS–Part 1: In-snow bromine activation and its impact on ozone, Atmos. Chem. Phys., 14, 4101–4133, doi:10.5194/acp-14-4101-2014, 2014.

Verwer, J. G., Spee, E. J., Blom, J. G., and Hundsdorfer, W.: Second-order Rosenbrock method applied to photochemical dispersion problems, SIAM J. Sci. Comput., 20, 1456–1480, 1999.

Wang, F., Saiz-Lopez, A., Mahajan, A. S., Gómez Martín, J. C., Armstrong, D., Lemes, M., Hay, T., and Prados-Roman, C.: Enhanced production of oxidized mercury over the tropical Pacific Ocean: a key missing oxidation pathway, Atmos. Chem. Phys., 14, 1323–1335, doi:10.5194/acp-14-1323-2014, 2014.

Weiss-Penzias, P., Jaffe, D. A., McClintick, A., Prestbo, E. M. and Landis, M. S.: Gaseous elemental mercury in the marine boundary layer: evidence for rapid removal in anthropogenic pollution, Environ. Sci. Technol., 37(17), 3755–3763, 2003.

Xie, Z.-Q., Sander, R., Pöschl, U., and Slemr, F.: Simulation of atmospheric mercury depletion events (AMDEs) during polar springtime using the MECCA box model, Atmos. Chem. Phys., 8, 7165–7180, doi: 10.5194/acp-8-7165-2008, 2008.

Zhang, L., Wright, L. P., and Blanchard, P.: A review of current knowledge concerning dry deposition of atmospheric mercury, Atmos. Environ., 43, 5853–5864, 2009.

Zhang, L., Blanchard, P., Gay, D. A., Prestbo, E. M., Risch, M. R., Johnson, D., Narayan, J., Zsolway, R., Holsen, T. M., Miller, E. K., Castro, M. S., Graydon, J. A., Louis, V. L. S., and Dalziel, J.: Estimation of speciated and total mercury dry deposition at monitoring locations in eastern and central North America, Atmos. Chem. Phys., 12, 4327–4340, 2012.

Table 1. Gas phase Hg reactions in the box model

No.	REACTIONS	KINETIC ($cm^3 molecule^{-1} s^{-1}$)	REFERENCE
G1	$Hg + O_3 \rightarrow HgO + O_2$	$8.43 \times 10^{-17} e^{-1407/T}$	Snider et al., 2008
G2	$Hg + OH \{+O_2\} \rightarrow HgO + HO_2$	$3.55 \times 10^{-14} e^{294/T}$	Pal and Ariya, 2004
G3	$Hg + H_2O_2 \rightarrow Hg(OH)_2$	8.5×10^{-19}	Tokos et al., 1998
G4	$Hg + Cl \rightarrow HgCl$	$6.4 \times 10^{-13} e^{(680 \times (1/T - 1/298))}$	Donohoue et al., 2005
G5	$Hg + Cl_2 \rightarrow HgCl_2$	2.6×10^{-18}	Ariya et al., 2002
G6	$Hg + Br \rightarrow HgBr$	$3.7 \times 10^{-13} (T/298)^{-2.76}$	Goodsite et al., 2004, 2012
G7	$Hg + BrO \rightarrow HgBrO$	1.8×10^{-14}	Raofie and Ariya, 2004
G8	$Hg + I \rightarrow HgI$	$4.0 \times 10^{-13} (T/298)^{-2.38}$	Goodsite et al., 2004
G9	$HgI \rightarrow Hg + I$	$3.0 \times 10^{9} e^{-3742/T}$	Goodsite et al., 2004
G10	$HgBr \rightarrow Hg + Br$	$1.6 \times 10^{-9} e^{-7801/T} \times [M]$	Dibble et al., 2012
G11	$HgBr + Br \rightarrow Hg + Br_2$	3.89×10^{-11}	Balabanov et al., 2005
G12	$HgBr + Br \rightarrow HgBr + Br$	3.97×10^{-11}	Balabanov et al., 2005
G13	$HgBr + Br \rightarrow HgBr_2$	2.98×10^{-11}	Balabanov et al., 2005
G14	$ClO + HgCl \rightarrow ClHgOCl$	5.0×10^{-11}	Dibble et al., 2012
G15	$ClO + HgBr \rightarrow BrHgOCl$	5.0×10^{-11}	Dibble et al., 2012
G16	$BrO + HgCl \rightarrow BrHgOCl$	1.09×10^{-10}	Dibble et al., 2012[1]
G17	$BrO + HgBr \rightarrow BrHgOBr$	1.09×10^{-10}	Dibble et al., 2012; Wang et al., 2014
G18	$NO_2 + HgCl \rightarrow ClHgNO_2$	8.6×10^{-11}	Dibble et al., 2012[1]
G19	$NO_2 + HgBr \rightarrow BrHgNO_2$	8.6×10^{-11}	Dibble et al., 2012; Wang et al., 2014
G20	$HO_2 + HgCl \rightarrow ClHgOOH$	8.2×10^{-11}	Dibble et al., 2012[1]
G21	$HO_2 + HgBr \rightarrow BrHgOOH$	8.2×10^{-11}	Dibble et al., 2012; Wang et al., 2014
G22	$OH + HgCl \rightarrow ClHgOH$	6.33×10^{-11}	Dibble et al., 2012[1]
G23	$OH + HgBr \rightarrow BrHgOH$	6.33×10^{-11}	Dibble et al., 2012; Wang et al., 2014
G24	$IO + HgBr \rightarrow BrHgOI$	4.9×10^{-11}	Wang et al., 2014

[1] The kinetic data of these HgCl reactions were not included in Dibble et al., 2012, they were assumed as the same kinetic as the HgBr reactions, which were calculated by Wang et al. (2014).

Table 2. Box model input and simulated variables.

Parameter	Appledore Island (AI)	Thompson Farm (TF)	Pack Monadnock (PM)
Observed[1]			
RH, relative humidity	76.9±5.4	69.9±19.5	69.0±13.1
Temperature, °C	19.1±1.7	21.3±4.3	18.5±3.3
[GEM], ppqv	133.9±3.3	138.4±12.8	149.6±3.2
[O_3], ppbv	37.4±8.8	32.7±15.7	45.0±4.2
[NO], pptv	154.5[2]	232.4±364.1	85.3±35.8
[CO], ppbv	169.6±13.9	156.2±10.8	120.2±7.2
Simulated[32]			
[Br], ppqv	28.50	0.20	0.18
[OH], ppqv	100.7	75.8	73.5
Other[43]			
v_d, cm s^{-1} , dry deposition velocity	GEM – 0.0045 GOM – 0.5 PBM – 0.5	GEM – 0.07 GOM – 1.2 PBM – 0.15	GEM – 0.08 GOM – 2.0 PBM – 0.25
H, M atm^{-1}, Henry's constants	$HgO - 3.2 \times 10^9$ $Hg(OH)_2 - 1.2 \times 10^7$ Other GOM $- 2.7 \times 10^9$	$HgO - 3.2 \times 10^9$ $Hg(OH)_2 - 1.2 \times 10^7$ Other GOM $- 2.7 \times 10^9$	$HgO - 3.2 \times 10^9$ $Hg(OH)_2 - 1.2 \times 10^7$ Other GOM $- 2.7 \times 10^9$
L, $m^3_{water} m^{-3}_{air}$, liquid water content	$5\sout{3} \times 10^{-11}$	$2.0\sout{1.25} \times 10^{-11}$	1.25×10^{-11}
D_g, $m^2 s^{-1}$, diffusion coefficient	1×10^{-5}	1×10^{-5}	1×10^{-5}
Z, m, boundary layer height	500	200 – 1120[54]	100
r_{dry}, µm, dry aerosol radius	3.5	0.3	0.07

[1] Observed 24-h mean values for all studied cases at these sites.
[2] Missing NO measurements at AI, use 154.5 ppqv for initial values.
[32] Simulated 24-h mean values for all studied days at these sites.
[43] Reference: Baumgardner et al., 2000; Kim et al., 2012; Mao and Talbot, 2004; Moldanová and Ljungström, 2001; Pillai and Moorthy, 2001; Shon et al., 2005; Zhang et al., 2009, 2012.
[54] TF boundary layer height changed at each hour, the averaged diurnal cycle was obtained from Research Data Archive at the National Center for Atmospheric Research, http://rda.ucar.edu/.

Table 3. Sensitivity ~~cases~~ scenarios with varying physical and chemical parameters. The superscript D represents daytime and N nighttime. Downward arrows stand for decreases and upward arrows increases. T stands for the temperature diurnal cycle in the base ~~case~~scenario, and T+10K or T-10K represents 10K higher temperature or 10K lower temperature throughout the day respectively.

~~Case~~Scenario No.	photolysis	Gas-droplet partitioning		Rate Coefficients (cm^3 $molec^{-1}$ s^{-1})			Temp.	Results	
		Include	Liquid water content ($m^3_{water} m^{-3}_{air}$)	GEM+O_3 (298K)	GEM+OH (298K)	GEM+Br (298K)		GOM	PBM
Base ~~Case~~Scenario									
0	Yes	Yes	5~~3~~.0E-11	7.5E-19[1]	9.5E-14[2]	3.7E-13[3]	T	--	--
Photochemistry									
1	No	Yes	~~3~~5.0E-11	7.5E-19	9.5E-14	3.7E-13	T	↓ ~~21~~3%-92~~80~~% ^{D}	↓ 2~~8~~-100~~92~~% ^{D}
Gas-particle partitioning									
2	Yes	No	--	7.5E-19	9.5E-14	3.7E-13	T	↑ ~280%	↓ 100%
Liquid water content									
3	Yes	Yes	3.0E-12	7.5E-19	9.5E-14	3.7E-13	T	↑ ~200%	↓ 80%
4	Yes	Yes	3.0E-10	7.5E-19	9.5E-14	3.7E-13	T	↓ 80~~7~~%	↑ ~~80~~50%
Reactions									
5	Yes	Yes	~~3~~5.0E-11	3.0E-20[4]	9.5E-14	3.7E-13	T	↓ 15% ^{D} ↓ 85~~0~~% ^{N}	↓49~~-5~~% ^{N}
6	Yes	Yes	~~3~~5.0E-11	--	9.5E-14	3.7E-13	T	↓ 1~~9~~6% ^{D} ↓88~~-92~~% ^{N}	↓ 51% ^{N}
7	Yes	Yes	~~3~~5.0E-11	7.5E-19	--	3.7E-13	T	↓ 10% ^{D}	Negligible
8	Yes	Yes	~~3~~5.0E-11	7.5E-19	9.5E-14	--	T	↓48~~-30~~% ^{D}	↓60~~-45~~% ^{D}
9	Yes	Yes	5.0E-11	7.5E-19	9.5E-14	3.2E-12[5]	T	↑ 250% ^{D}	↑ 300%
Temperature									
10~~9~~	Yes	Yes	~~3~~5.0E-11	7.5E-19	9.5E-14	3.7E-13	T+10K	↓ 9% ^{D} ↑ 13% ^{N}	↓ 9% ^{D} ↑ 54% ^{N}
11~~0~~	Yes	Yes	~~3~~5.0E-11	7.5E-19	9.5E-14	3.7E-13	T-10K	↑ 9% ^{D} ↓ 11% ^{N}	↑ 8% ^{D} ↓ 28% ^{N}

[1] Snider et al., 2008; [2] Pal and Ariya, 2004; [3] Goodsite et al., 2004, 2012; [4] Hall, 1995; [5] Ariya et al., 2002.

Table 4. Possible pathways of BrO + CH_3O_2 reaction

NO.	Reactions	Kinetics ($cm^3molecule^{-1}s^{-1}$)	Reference
B1	$BrO(g) + CH_3O_2(g) \rightarrow CH_3O(g) + BrOO(g)$ $BrOO(g) \rightarrow Br(g) + O_2(g)$	1.4×10^{-12} Fast	Aranda et al., 1997; Atkinson et al., 2008
B2	$BrO(g) + CH_3O_2(g) \rightarrow CH_2O_2(g) + HOBr(g)$	4.3×10^{-12}	Aranda et al., 1997; Atkinson et al., 2008
B3	$BrO(g) + CH_3O_2(g) \rightarrow CH_3OBr(g) + O_2(g)$	?	Aranda et al., 1997
B4	$BrO(g) + CH_3O_2(g) \rightarrow CH_3OOOBr(g) \rightarrow CH_2O(g) + HOOBr(g)$	?	Guha and Francisco, 2003

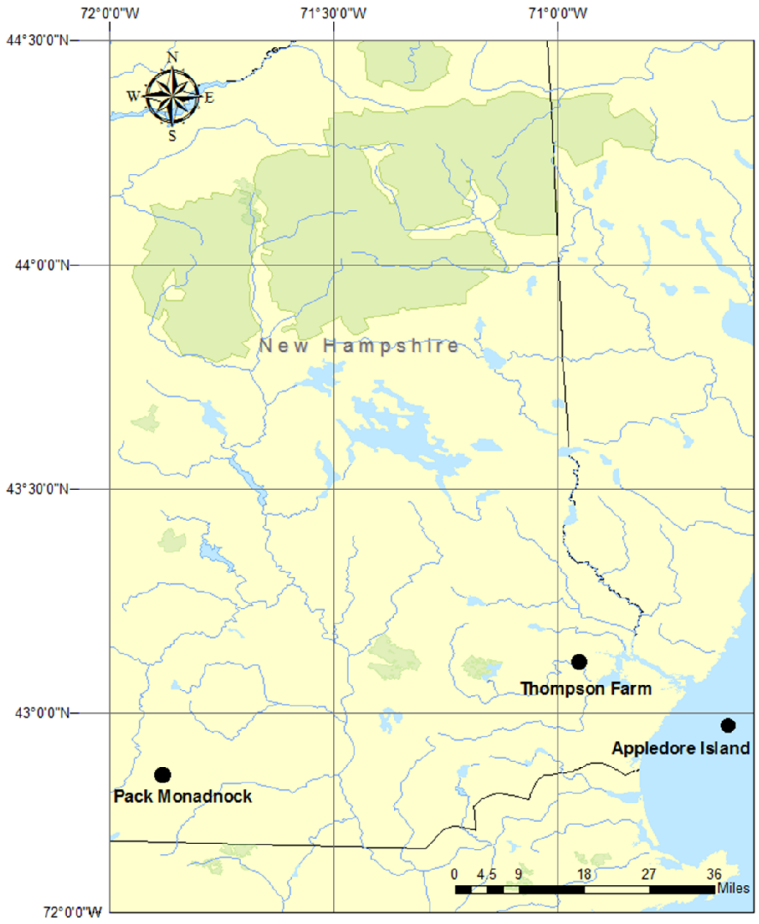

Figure 1. New Hampshire site map: Appledore Island (marine), Thompson Farm (coastal), and Pack Monadnock (inland elevated).

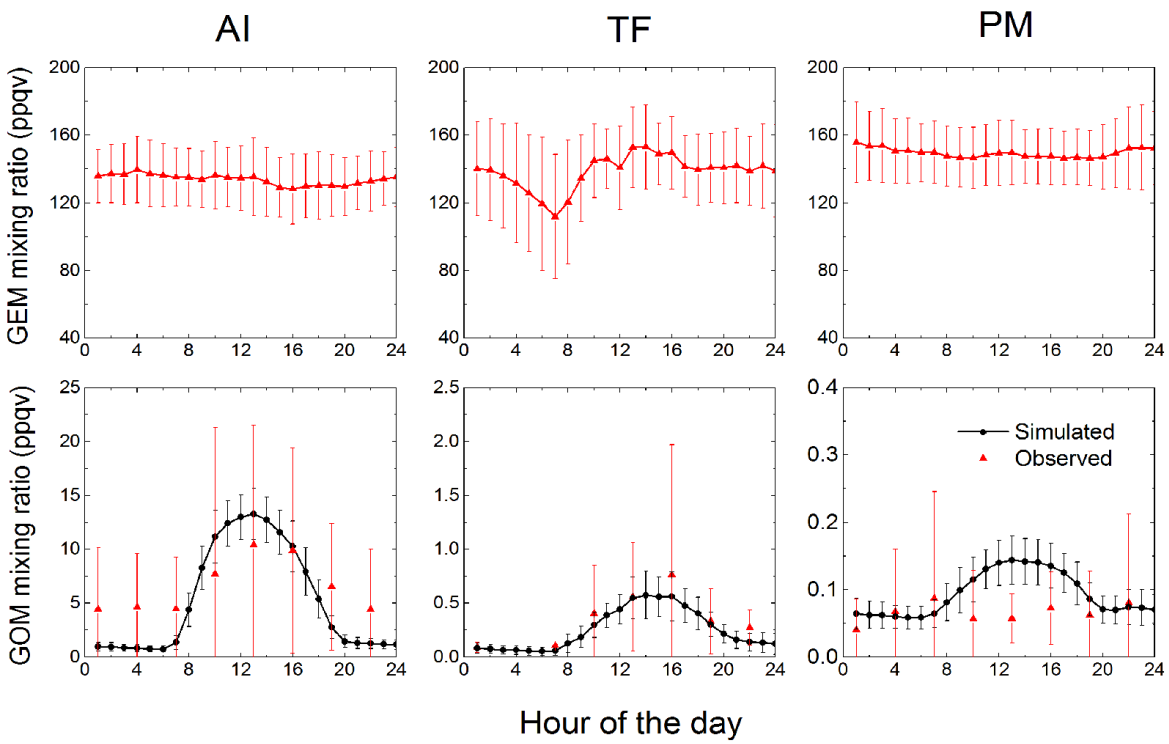

Figure 2. Average diurnal cycles ~~and whisker diagrams~~ of observed ~~GOM and~~ GEM ~~observations~~(top panel) and simulated and observed GOM (bottom panel) averaged over the selected 50 days at Appledore Island (AI), 12 days at Thompson Farm (TF), and 21 days at Pack Monadnock (PM) from summers of 2007, 2008, and 2010. The error bars represent standard deviation.

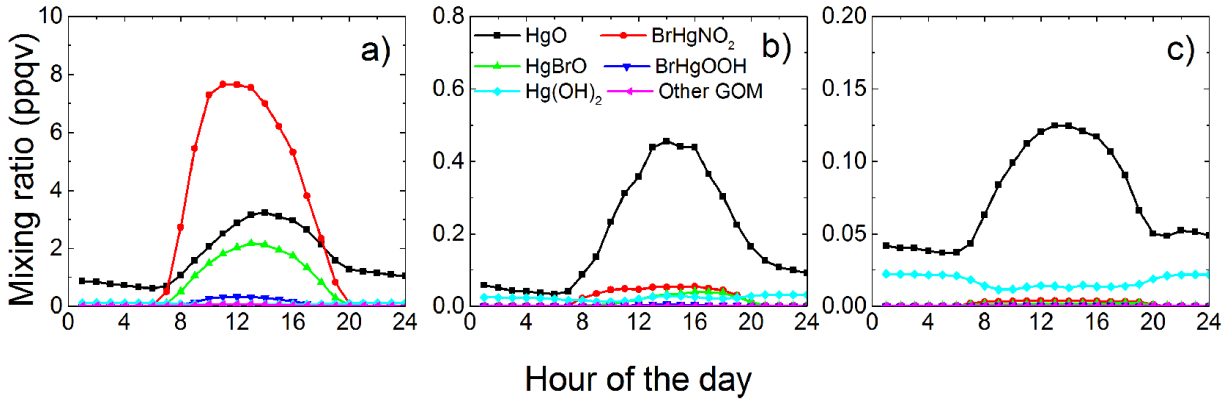

Figure 43. Simulated average diurnal cycles of GOM speciation at AI (a), TF (b), and PM (c).

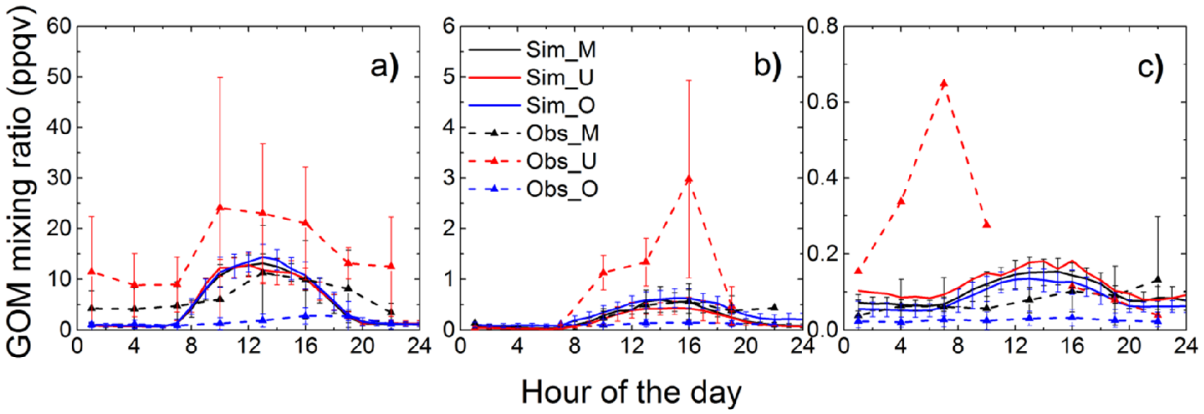

Figure 4. Observed (dash line with scatters) and simulated (solid line) average diurnal cycles of GOM for the matching (black, "Sim_M" and "Obs_M"), under-estimation (red, "Sim_U" and "Obs_U"), and over-estimation cases (blue, "Sim_O" and "Obs_O") at AI (a), TF (b), and PM (c). The bars represent the standard deviations at each hour for those specific days.

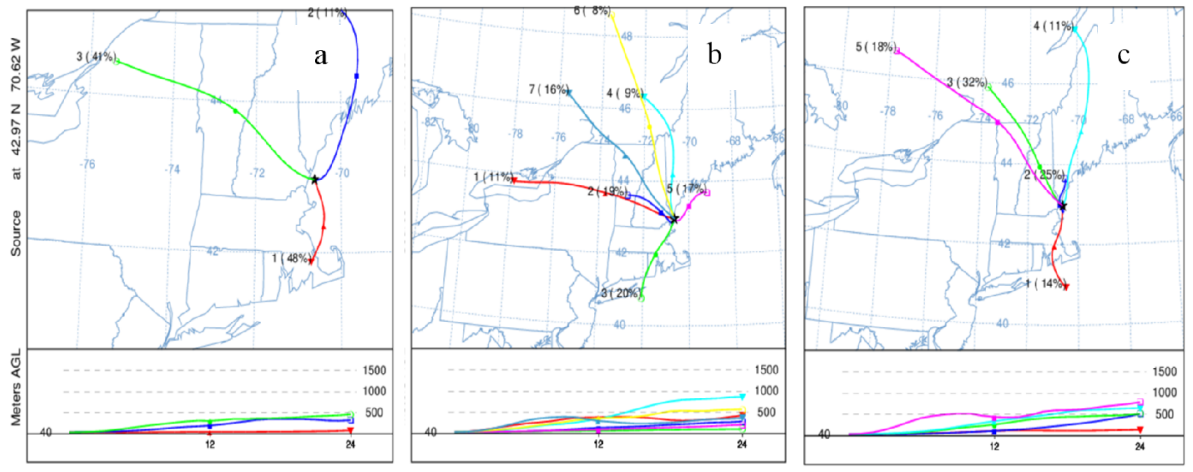

Figure 5. Clustered 24-hours back trajectories of air masses in (a) over-estimation cases, (b) matching cases, and (c) under-estimation cases at AI.

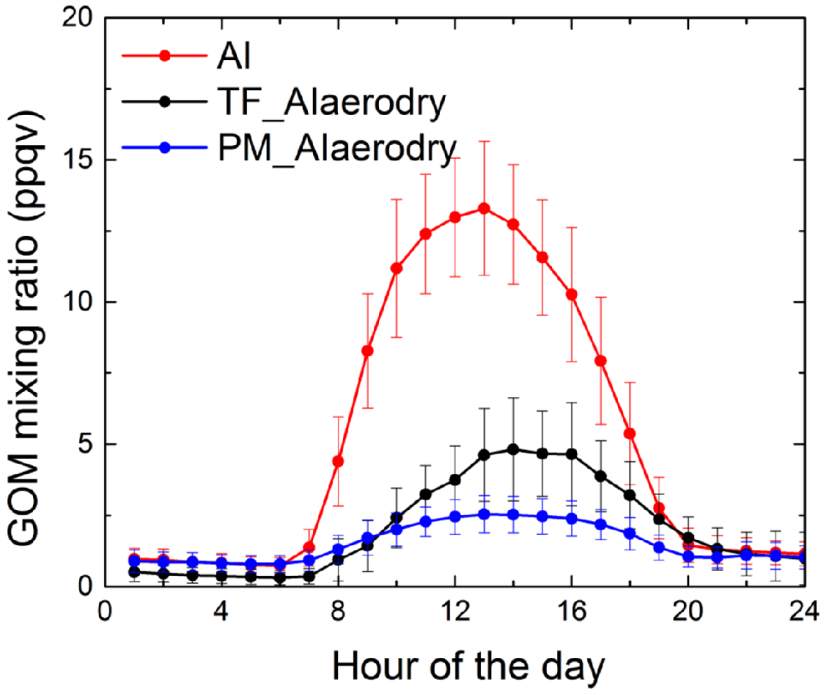

Figure ~~5~~6. Simulated averaged diurnal cycles of GOM at AI (red), at TF (black~~blue~~) using AI dry deposition and gas-aerosol partitioning parameters ("TF_AIaerodry"), and at PM (blue~~green~~) using AI dry deposition and gas-to-particle partitioning parameters ("PM_AIaerodry").

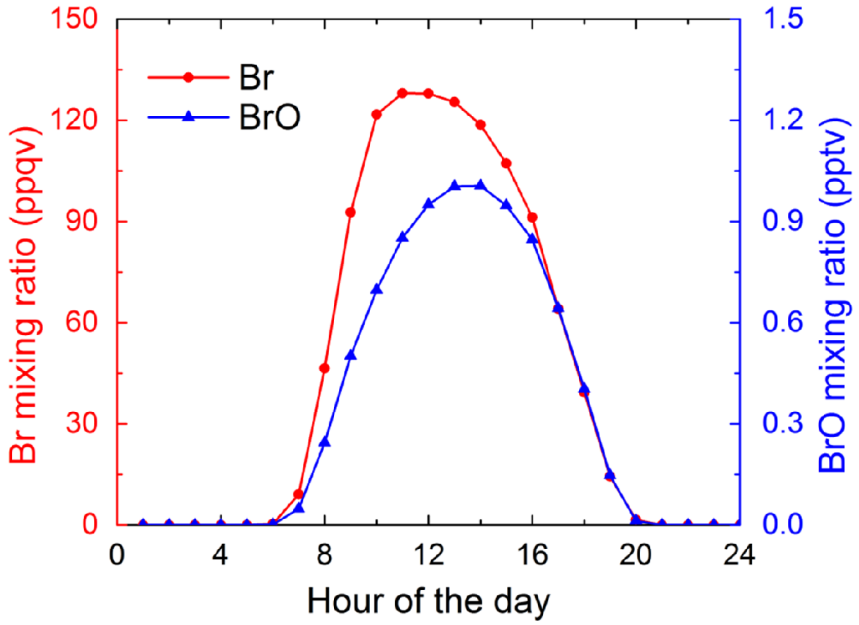

Figure ~~6~~7. Simulated diurnal cycles of Br (red) and BrO (blue) of the base case.

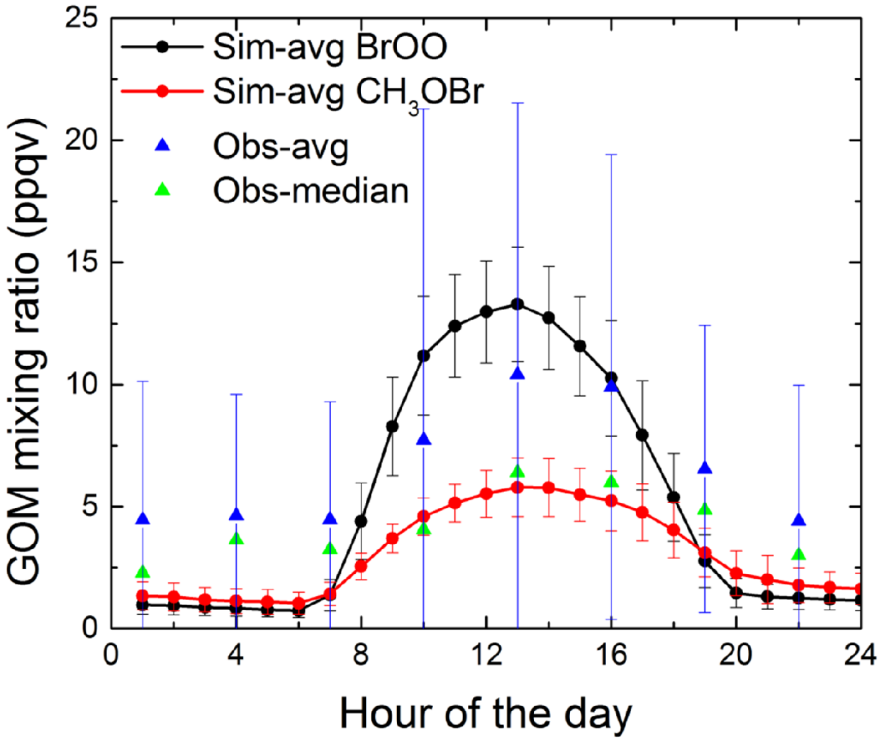

Figure ~~7~~8. Simulated average diurnal cycles of GOM for the base ~~case~~ scenario ("Sim-avg BrOO", black circle) and for the "CH_3OBr" ~~case~~ scenario ("Sim-avg CH_3OBr", red, circle), observed average GOM diurnal cycle ("Obs-avg", blue, triangle scatter), and observed median GOM diurnal cycle ("Obs-median", green, triangle scatter) of the 50 cases at AI.

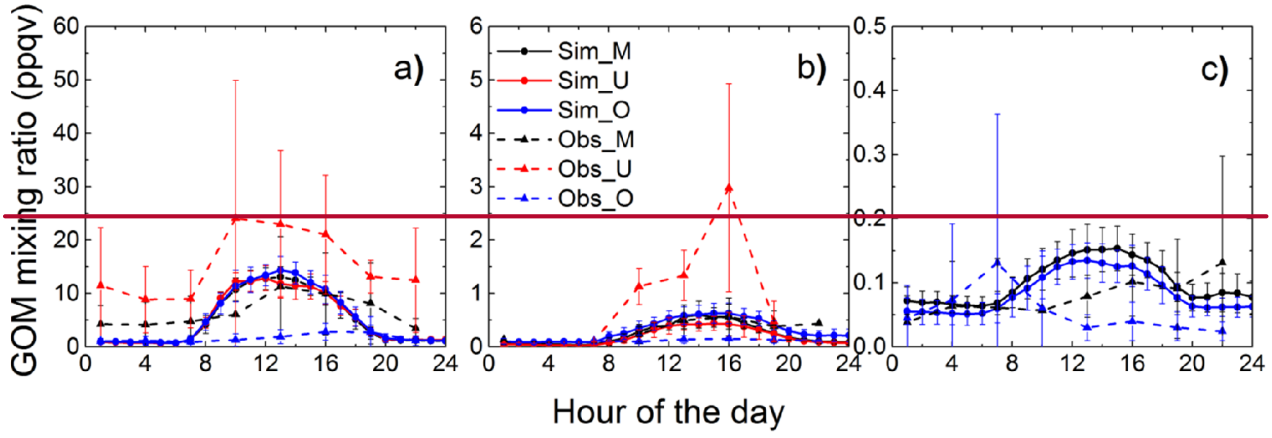

~~Figure 9. Observed (solid line) and simulated (dash line) average diurnal cycles of GOM for the matching (red), under-estimation (blue), and over-estimation cases (green) at AI (a), TF (b), and PM (c). The bars represent the minimum and maximum mixing ratios at each hour for those specific days.~~

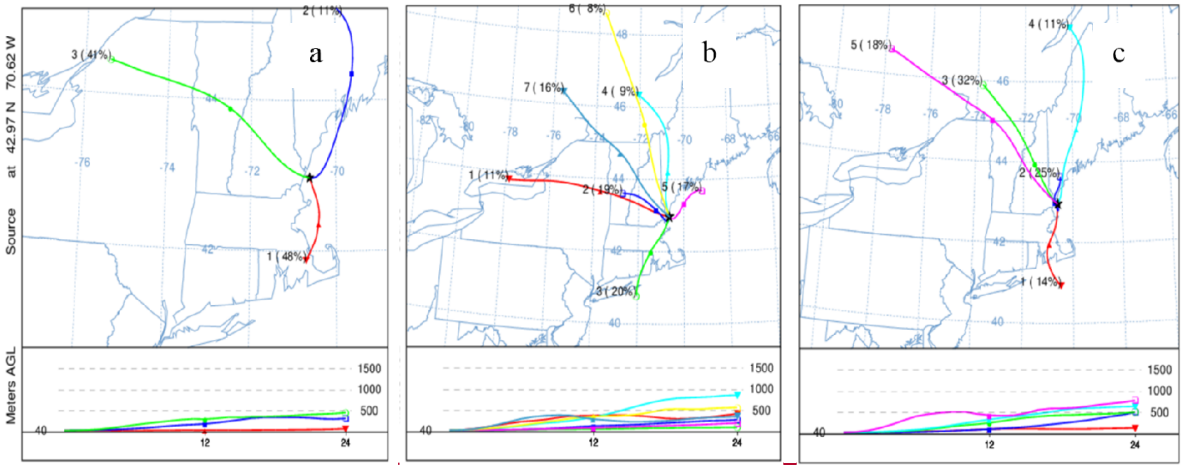

~~Figure 10. Clustered 24-hours back trajectories of air masses in (a) over-estimation cases, (b) match cases, and (c) under-estimation cases at AI.~~

Table S1. Aqueous phase reactions and equilibriums of Hg in the box model.

No.	REACTIONS	KINETIC (L mol^{-1} s^{-1}) or EQUILIBRIUM CONSTANT	REFERENCE
A1	Hg^0 (aq) + O_3 (aq) → HgO (aq) + O_2 (aq)	2.4×10^9	Munthe et al., 1992
A2	Hg^0 (aq) + OH (aq) → HgOH (aq)	2.4×10^9	Gardfeldt et al., 2001
A3	HgOH (aq) + OH (aq) → $Hg(OH)_2$ (aq)	1.0×10^{10}	Nazhat and Asmus, 1973
A4	HgOH (aq) + O_2 (aq) + H_2O (aq) → $Hg(OH)_2$ (aq) + H^+ + O_2^-	1.0×10^9	Nazhat and Asmus, 1973
A5	Hg^0 (aq) + OH (aq) → Hg^+ + OH^-	2.0×10^9	Lin and Pehkonen, 1997

A6	$HgO\ (aq) + H^+ \rightarrow Hg^{2+} + OH^-$	1.0×10^{10}	Pleijel and Munthe, 1995
A7	$HOCl\ (aq) + Hg^0\ (aq) \rightarrow Hg^{2+} + Cl^- + OH^-$	2.09×10^{6}	Lin and Pehkonen, 1997
A8	$ClO^- + Hg^0\ (aq) \rightarrow Hg^{2+} + Cl^- + OH^-$	1.99×10^{6}	Lin and Pehkonen, 1997
A9	$HgSO_3\ (aq) \rightarrow Hg^0\ (aq) + S(VI)$	0.6	Munthe et al., 1991
A10	$Hg(OH)_2\ (aq) \rightarrow Hg^0\ (aq) + products$	3.0×10^{7}	Pleijel and Munthe, 1995
A11	$Hg^+ + HO_2\ (aq) \rightarrow Hg^0\ (aq) + O_2\ (aq) + H^+$	1.0×10^{10}	Xie et al., 2008
A12	$Hg^{2+} + HO_2\ (aq) \rightarrow Hg^+ + O_2\ (aq) + H^+$	1.7×10^{4}	Pehkonen and Lin, 1998
AE1	$Hg^{2+} + SO_3^{2-} \leftrightarrow HgSO_3\ (aq)$	2.0×10^{13}	van Loon et al., 2001
AE2	$HgSO_3\ (aq) + SO_3^{2-} \leftrightarrow Hg(SO_3)_2^{2-}$	1.0×10^{10}	van Loon et al., 2001
AE3	$Hg^{2+} + OH^- \leftrightarrow HgOH^+$	3.98×10^{10}	Smith and Martell, 2004
AE4	$HgOH^+ + OH^- \leftrightarrow Hg(OH)_2\ (aq)$	1.58×10^{11}	Smith and Martell, 2004
AE5	$HgOH^+ + Cl^- \leftrightarrow HgOHCl\ (aq)$	2.7×10^{7}	Xiao, 1994
AE6	$Hg^{2+} + Cl^- \leftrightarrow HgCl^+$	2.0×10^{7}	Smith and Martell, 2004
AE7	$HgCl^+ + Cl^- \leftrightarrow HgCl_2\ (aq)$	5.0×10^{6}	Smith and Martell, 2004
AE8	$HgCl_2\ (aq) + Cl^- \leftrightarrow HgCl_3^-$	6.7	Smith and Martell, 2004
AE9	$HgCl_3^- + Cl^- \leftrightarrow HgCl_4^{2-}$	13.0	Smith and Martell, 2004
AE10	$Hg^{2+} + Br^- \leftrightarrow HgBr^+$	1.10×10^{9}	Smith and Martell, 2004
AE11	$HgBr^+ + Br^- \leftrightarrow HgBr_2\ (aq)$	2.50×10^{8}	Smith and Martell, 2004
AE12	$HgBr_2\ (aq) + Br^- \leftrightarrow HgBr_3^-$	1.50×10^{2}	Smith and Martell, 2004
AE13	$HgBr_3^- + Br^- \leftrightarrow HgBr_4^{2-}$	23.0	Smith and Martell, 2004

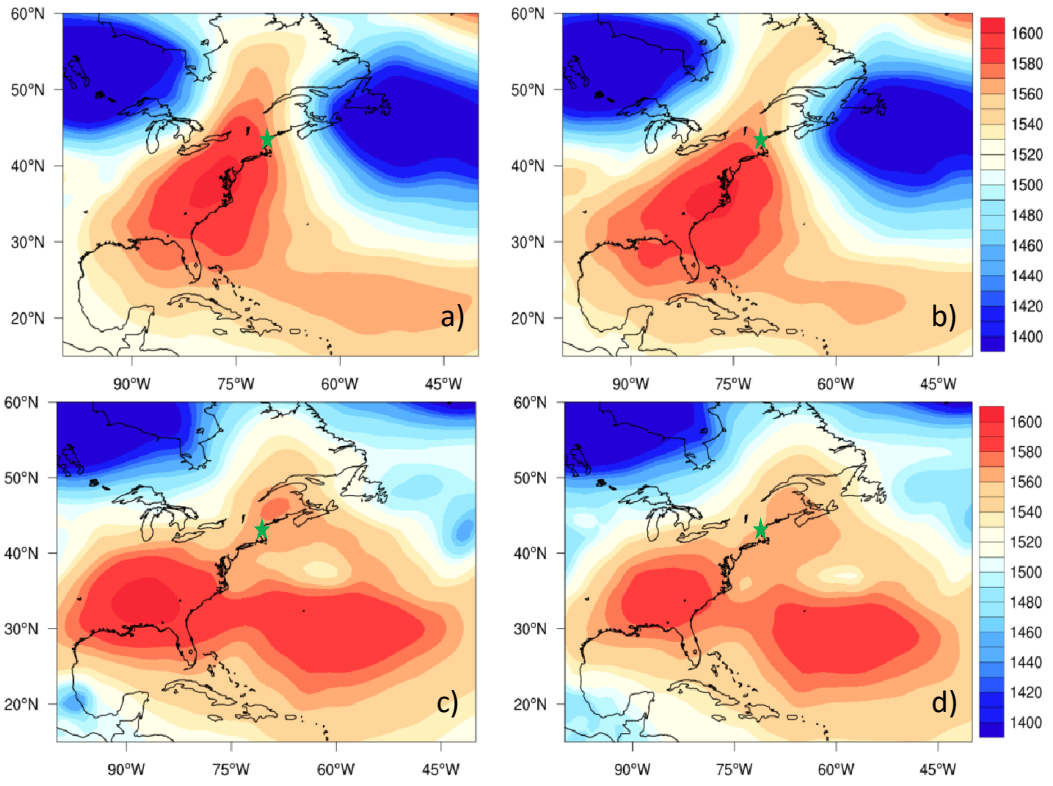

Figure S1. Geopotential height for a) 06/13/2008 08:00 EDT, b) 06/13/2008 14:00 EDT, c) 08/22/2007 14:00 EDT, and d) 08/22/2007 20:00 EDT at 850 hPa, the green star shows the location of TF site.